# Quasi-Symmetric Nets: A Constructive Approach to the Equimodular Elliptic Type of Kokotsakis Polyhedra

A. Nurmatov<sup>a</sup>, M. Skopenkov<sup>a</sup>, F. Rist<sup>a</sup>, J. Klein<sup>a</sup>, D. L. Michels<sup>a,\*</sup>

<sup>a</sup>KAUST Computational Sciences Group, Campus Building 1, Thuwal, 23955-6900, KSA

## **Abstract**

This work investigates flexible Kokotsakis polyhedra with a quadrangular base of equimodular elliptic type, filling a significant gap in the literature by providing the first explicit constructions of this type together with an explicit algebraic characterization in terms of flat and dihedral angles. A straightforwardly constructible class of polyhedra – called quasi-symmetric nets (QSnets) – is introduced, characterized by a symmetry relation among flat angles. It is shown that every elliptic QS-net has equimodular elliptic type and is flexible in real three-dimensional Euclidean space (rather than only in complex configuration spaces), except for a few exceptional choices of dihedral angles, and that its flexion admits a closed-form parameterization. Examples are constructed that are non-self-intersecting and belong exclusively to the equimodular elliptic type. To support applications in computational geometry, a numerical pipeline is developed that searches for candidate solutions, verifies them using the explicit algebraic characterization, and constructs and visualizes the resulting polyhedra; numerical validations achieve high precision. Taken together, these results provide constructive criteria, algorithms, and validated examples for the equimodular elliptic type, enabling the design of a broad range of flexible Kokotsakis mechanisms.

Keywords: Equimodular elliptic class, elliptic function, explicit

<sup>\*</sup>Corresponding author

Email addresses: abdukhomid.nurmatov@kaust.edu.sa (A. Nurmatov), mikhail.skopenkov@gmail.com (M. Skopenkov), florian.rist@kaust.edu.sa (F. Rist), jonathan.klein@kaust.edu.sa (J. Klein), dominik.michels@kaust.edu.sa (D. L. Michels)

## 1. Introduction and Prior Work

The increasing interest in flexible and deployable structures stems from their broad utility across fields like robotics, solar cells, meta-materials, art, and architecture. In architecture, these structures simplify construction, enable innovative designs, and enhance building functionality. Notable examples include Santiago Calatrava Valls' projects such as the Florida Polytechnic University, the UAE Pavilion at Expo Dubai, and the Quadracci Pavilion in Milwaukee. Norman Foster's Bund Finance Center also showcases such principles. While architects typically rely on simple mechanisms, we explore a wider range of mechanisms with potential for architectural design. Unlike traditional kinematic frame structures (see [1]-[3]), our flexible polyhedra mechanisms enable full surface coverage, making them suitable for diverse applications. Such deployable structures, particularly those that transition into flat or curved shapes, are gaining attention for their potential to optimize construction. Recent work includes rigid-foldable origami (see [4]–[13]) and programmable meta-materials (see [14]–[20]), which often involve mechanisms with multiple degrees of freedom.

The study of flexible polyhedra – polyhedral structures capable of continuous isometric deformations while their faces remain rigid – has long been an active area of research at the interface of geometry, kinematics, and mechanics. Interest in such mechanisms is driven both by their intrinsic mathematical appeal and by their applications in architectural geometry, deployable structures, and origami-inspired design. Since Cauchy's classical rigidity theorem [21] established that convex polyhedra are rigid, research has focused on identifying and characterizing non-convex configurations that admit flexibility. Bricard's seminal classification of flexible octahedra [22] not only revealed the existence of such extraordinary mechanisms but also introduced algebraic methods that remain central to the field.

Within this context, Kokotsakis polyhedra form one of the most fundamental families of flexible mechanisms, named after Antonios Kokotsakis, who first studied them in the 1930s [23]. A Kokotsakis polyhedron is a polyhedral surface in  $\mathbb{R}^3$  consisting of one n-gon (the base), n quadrilaterals attached to each side of the n-gon, and n triangles placed between every two consecutive quadrilaterals. See Figure 1. While generically rigid, certain

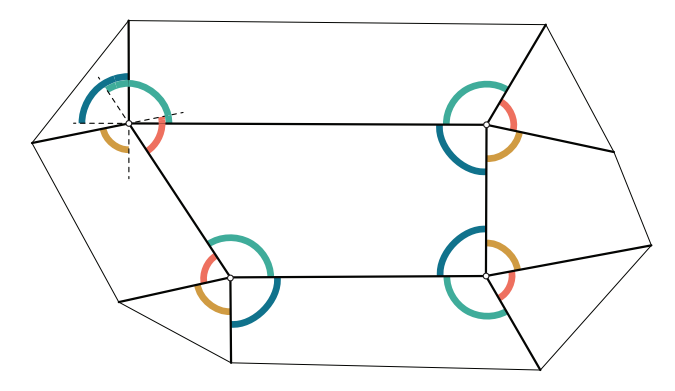


Figure 1: A QS-net is a particular Kokotsakis polyhedron with quadrangular base. The flat angles of the same color are equal. Such a net is generically flexible.

configurations of Kokotsakis polyhedra admit continuous flexion. Kokotsakis derived necessary and sufficient conditions for infinitesimal flexibility and described several flexible subclasses.

The quadrangular case (n=4) has been the subject of extensive investigation, starting with early contributions by Sauer and Graf [24] and later by Stachel and collaborators (see [25]–[27]), who employed resultant-based algebraic methods to classify several subclasses. Infinitesimal flexibility was addressed by Bobenko, Hoffmann, Schief [28], and Karpenkov [29]. The culmination of this line of work is the comprehensive classification by Izmestiev [30], who established eight principal classes of flexible Kokotsakis polyhedra and showed that every flexible quadrangular Kokotsakis polyhedron belongs to one of them (possibly after switching boundary strips): orthodiagonal, isogonal, equimodular, conjugate-modular, linear compound, linearly conjugate, chimera, and trivial class.

Since the classification of flexible polyhedra is complicated [31], it is natural to search for polyhedra that are approximately flexible with high tolerance, which is enough for any practical applications. Beautiful examples were constructed by Gor'kavyi and Milka [32]. A general approach was developed in a recent series of papers [33]–[36], in which approximately flexible polyhedra were constructed by optimizing their analogs in isotropic geometry.

The detailed investigation of Izmestiev's classes is ongoing. Each class in Izmestiev's framework is subdivided into subclasses, and several open questions remain unresolved. First, it is not guaranteed that every subclass contains realizable examples (flexible Kokotsakis polyhedra). Second, even when examples exist, flexibility is often established only in  $\mathbb{C}^3$ , not neces-

sarily in  $\mathbb{R}^3$ . Third, realizable examples in  $\mathbb{R}^3$  may self-intersect, raising the question of if each subclass admits non-self-intersecting flexible polyhedra. Finally, since some classes intersect with each other, an important question is if there exist examples belonging exclusively to a given class. Addressing these questions begins with constructing explicit examples within each class.

Progress has been made in several directions. The orthodiagonal involutive type, first studied by Sauer and Graf [24] as the *T-surfaces*, or *T-nets*, and the orthodiagonal antiinvolutive type, analyzed by Erofeev and Ivanov [37], provide explicit examples and parametrizations within the orthodiagonal class, confirming conjectures posed by Stachel. Recent work has extended this class to Kokotsakis meshes with skew (non-planar) faces, see Aikyn et al. [38] and Liu et al. [31]. Flexible polyhedra of the isogonal class were also identified in [24] as discrete Voss surfaces, or V-nets. These advances have yielded examples for the first two classes (orthodiagonal and isogonal) in Izmestiev's classification. However, until now, no explicit examples have been known for the third class, the equimodular type.

This paper focuses on the equimodular elliptic type, a subclass of the equimodular class identified by Izmestiev [30]. This subclass is defined in terms of Jacobi elliptic functions and believed to have the maximal number of degrees of freedom. Our work contributes new constructive and analytical results, thereby advancing the understanding and practical realization of this class of flexible mechanisms and addressing the open problems described above. For the first time, we present an explicit construction of such polyhedra, thereby demonstrating that the equimodular elliptic class is non-empty. Namely, we introduce an easily constructible class of quasi-symmetric nets, or QS-nets, defined by equality and complementarity (to  $\pi$ ) of certain flat angles as shown in Figure 1. In Theorem 1, we show that under a simple additional condition (ellipticity), all QS-nets belong to the equimodular elliptic class, are flexible in  $\mathbb{R}^3$  besides a few exceptional values of dihedral angles, and admit a simple closed-form expression for the flexion.

Furthermore, we introduce a construction with the dihedral rather than flat angles as design parameters, allowing for better control of the visual appearance of polyhedra. In Proposition 1, we derive an algebraic characterization of equimodular elliptic type in terms of flat and dihedral angles.

Beyond existence, we give examples that are flexible in  $\mathbb{R}^3$ , are non-self-intersecting, and belong exclusively to the equimodular elliptic type, even after switching boundary strips. We further use Proposition 1 to obtain numerical examples with tolerance  $10^{-12}$  or better, sufficient for applications in

real-world mechanism design. To complement the theoretical developments, we introduce computational algorithms that (i) search for and verify candidate solutions to the existence system with desired tolerance, (ii) construct and visualize the resulting polyhedra with interactive flexion, and (iii) guide the physical construction of models.

In summary, the contributions of this work are:

- the construction of the first explicit closed-form examples of flexible (in  $\mathbb{R}^3$ ), non-self-intersecting polyhedra that belong exclusively to equimodular elliptic type;
- an explicit algebraic characterization of equimodular elliptic type;
- the development of numerical algorithms for search, verification, and visualization of such polyhedra;
- the construction of the numerical examples of polyhedra of equimodular elliptic type with desired tolerance.

The paper is organized as follows. Section 2 introduces the necessary notation and states the main results, Theorem 1 and Proposition 1. Section 3 contains the proofs of these results. Section 4 presents the numerical search algorithm and reports closed-form and numerical examples. Section 5 discusses implications for further research on flexible polyhedra and potential CAD applications. A brief conclusion in Section 6 closes the paper.

#### 2. Notation and Main Results

Let us introduce the main notions, notation, and state the main results. An  $m \times n$  net (with convex faces) is a collection of (m+1)(n+1) points  $V_{ij} \in \mathbb{R}^3$ , indexed by integers  $0 \le i \le m$  and  $0 \le j \le n$  such that, for all  $0 \le i < m$  and  $0 \le j < n$ , the points  $V_{ij}, V_{i+1,j}, V_{i+1,j+1}, V_{i,j+1}$  form the consecutive vertices of a convex quadrilateral, denoted  $F_{ij}$ . See Figure 2. (See [39] for an elementary introduction to indexed/labeled polyhedra.)

An  $m \times n$  net  $V_{ij}$  is flexible (in  $\mathbb{R}^3$ ) if belongs to a continuous family (called flexion) of  $m \times n$  nets  $V_{ij}(t)$ , where  $t \in (-\epsilon, \epsilon)$  for some  $\epsilon > 0$ , such that all corresponding quadrilaterals  $F_{ij}(t)$  are congruent to  $F_{ij}(0)$  for all  $t \in (-\epsilon, \epsilon)$ ,  $V_{ij}(0)$  is the original net  $V_{ij}$ , and the nets  $V_{ij}(t)$  are pairwise non-congruent.

In what follows, we consider only  $3\times3$  nets and call them simply *polyhedra*. We omit corner points  $V_{00}$ ,  $V_{30}$ ,  $V_{03}$ , and  $V_{33}$ , irrelevant for the flexibility.

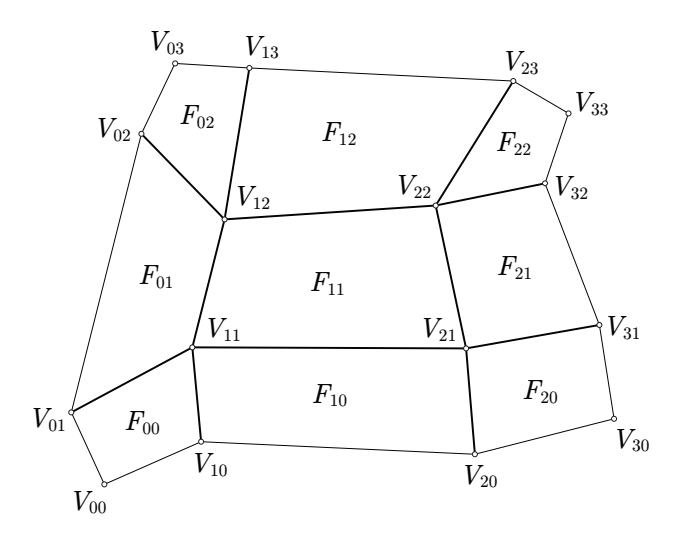


Figure 2: Illustration of a  $3 \times 3$  net.

We denote the vertices  $A_2 := V_{11}$ ,  $B_2 := V_{10}$ ,  $C_2 := V_{01}$ , etc. as shown in Figure 3. Denote also  $A_0 := A_4$  and  $A_5 := A_1$ . By flat angles of the  $3 \times 3$  net we mean  $\alpha_i = \angle A_{i-(-1)^i}A_iB_i$ ,  $\beta_i = \angle B_iA_iC_i$ ,  $\gamma_i = \angle C_iA_iA_{5-i}$ ,  $\delta_i = \angle A_{i-1}A_iA_{i+1}$ , where  $i = 1, \ldots, 4$ . By definition,  $\alpha_i$ ,  $\beta_i$ ,  $\gamma_i$ ,  $\delta_i \in (0, \pi)$ .

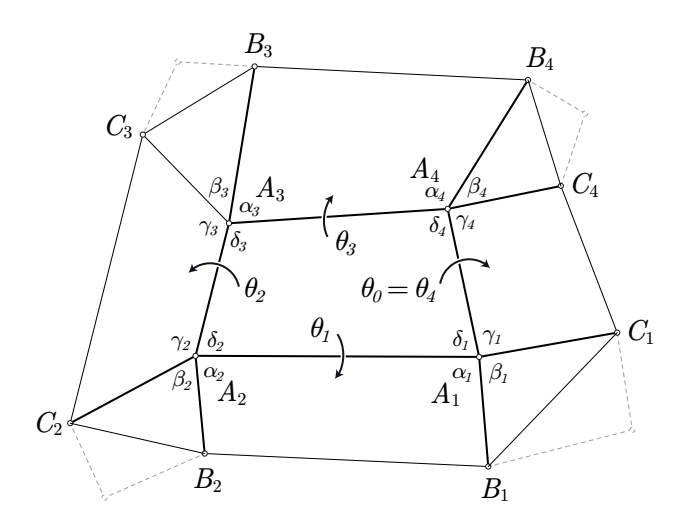


Figure 3: Notation for the vertices, flat and dihedral angles of a  $3 \times 3$  net without corners.

Introduce oriented normals 
$$\overrightarrow{n_0} := \overrightarrow{A_2A_1} \times \overrightarrow{A_2A_3}, \overrightarrow{n_1} := \overrightarrow{A_2B_2} \times \overrightarrow{A_2A_1},$$
  
 $\overrightarrow{n_2} := \overrightarrow{A_2A_3} \times \overrightarrow{A_2C_2}, \overrightarrow{n_3} := \overrightarrow{A_3A_4} \times \overrightarrow{A_3B_3}, \overrightarrow{n_4} := \overrightarrow{A_1C_1} \times \overrightarrow{A_1A_4}.$  For each

 $i=1,\ldots,4$ , the (oriented) dihedral angle of the  $3\times 3$  net is defined as

$$\theta_i := \begin{cases} \angle \left(\overrightarrow{n_0}, \overrightarrow{n_i}\right) \in (0, \pi), & \text{if } \det \left(\overrightarrow{n_i}, \overrightarrow{n_0}, \overrightarrow{A_{i+1}A_i}\right) > 0, \\ -\angle \left(\overrightarrow{n_0}, \overrightarrow{n_i}\right) \in [-\pi, 0], & \text{if } \det \left(\overrightarrow{n_i}, \overrightarrow{n_0}, \overrightarrow{A_{i+1}A_i}\right) \le 0. \end{cases}$$

Although the theoretical framework presented is valid for dihedral angles in the full range  $[-\pi, \pi)$ , we consider the case where  $\theta_i \in (0, \pi)$ , unless otherwise explicitly indicated. Furthermore, we define  $\theta_0 := \theta_4$  (see Figure 3).

**Definition 1.** A  $3 \times 3$  net is *quasi-symmetric*, or a *QS-net*, if its flat angles satisfy the relations (see Figure 1)

$$\alpha_1 = \alpha_4 = \delta_2 = \pi - \delta_3, \qquad \beta_1 = \beta_4 = \gamma_2 = \pi - \gamma_3, 
\gamma_1 = \gamma_4 = \beta_2 = \pi - \beta_3, \qquad \delta_1 = \delta_4 = \alpha_2 = \pi - \alpha_3.$$
(1)

A polyhedron has *elliptic type* if

$$\alpha_i \pm \beta_i \pm \gamma_i \pm \delta_i \neq 0 \pmod{2\pi} \tag{2}$$

for all choices of the signs  $\pm$  and each  $i=1,\ldots,4$ . In what follows, we consider polyhedra of elliptic type only, unless otherwise explicitly indicated, and call them *elliptic polyhedra*. We introduce the notation:

$$\sigma_{i} := \frac{\alpha_{i} + \beta_{i} + \gamma_{i} + \delta_{i}}{2}, \quad \overline{\alpha}_{i} := \sigma_{i} - \alpha_{i}, \quad \overline{\beta}_{i} := \sigma_{i} - \beta_{i}, 
\varepsilon_{i} := \operatorname{sgn}(\sin \sigma_{i}), \qquad \overline{\gamma}_{i} := \sigma_{i} - \gamma_{i}, \quad \overline{\delta}_{i} := \sigma_{i} - \delta_{i}.$$
(3)

Next, we define

$$a_{i} := \frac{\sin \alpha_{i}}{\sin \overline{\alpha}_{i}}, \qquad b_{i} := \frac{\sin \beta_{i}}{\sin \overline{\beta}_{i}}, \quad c_{i} := \frac{\sin \gamma_{i}}{\sin \overline{\gamma}_{i}}, \quad d_{i} := \frac{\sin \delta_{i}}{\sin \overline{\delta}_{i}},$$

$$M_{i} := a_{i} b_{i} c_{i} d_{i}, \quad r_{i} := a_{i} d_{i}, \quad s_{i} := c_{i} d_{i}, \quad f_{i} := a_{i} c_{i},$$

$$u_{i} := 1 - M_{i}, \quad x_{i} := \frac{1}{r_{i} - 1}, \quad y_{i} := \frac{1}{s_{i} - 1}, \quad z_{i} := \frac{1}{f_{i} - 1}.$$

$$(4)$$

A polyhedron has *equimodular elliptic type* if it has elliptic type and the following three conditions hold:

(1) The vertices have equal moduli, that is,

$$M_1 = M_2 = M_3 = M_4 := M. (5)$$

(2) The amplitudes at common vertices match, that is,

$$r_1 = r_2, \quad s_1 = s_4, \quad r_3 = r_4, \quad s_2 = s_3.$$
 (6)

(3) The sum of *phase shifts* is a *period*, that is, for some  $e_1$ ,  $e_2$ ,  $e_3 \in \{+1, -1\}$  we have

$$t_1 + e_1 t_2 + e_2 t_3 + e_3 t_4 \in \Lambda. (7)$$

In the latter equation, we use the following notation. First, we introduce the  $elliptic\ modulus$ 

$$k := \begin{cases} \sqrt{1 - M}, & \text{if } M < 1, \\ \sqrt{1 - M^{-1}}, & \text{if } M > 1. \end{cases}$$
 (8)

The basis quater periods are

$$K := K(k) = \int_0^1 \frac{dx}{\sqrt{(1 - x^2)(1 - k^2 x^2)}},$$

$$K' := K(k') = \int_0^1 \frac{dx}{\sqrt{(1 - x^2)(1 - k'^2 x^2)}},$$
(9)

where  $k' = \sqrt{1 - k^2}$ . Then we introduce the lattice

$$\Lambda := \begin{cases} \{4Km + 2\mathbf{i}K'n : m, n \in \mathbb{Z}\}, & \text{if } M < 1, \\ \{4Km + (2K + 2\mathbf{i}K')n : m, n \in \mathbb{Z}\}, & \text{if } M > 1, \end{cases}$$

where  $\mathbf{i}$  (in bold font) is the imaginary unit.

The amplitudes  $p_i$  and  $q_i$  are given by

$$p_i := \sqrt{r_i - 1} \in \mathbb{R}_{>0} \cup \mathbf{i} \mathbb{R}_{>0}, \quad q_i := \sqrt{s_i - 1} \in \mathbb{R}_{>0} \cup \mathbf{i} \mathbb{R}_{>0}.$$
 (10)

Finally, the *phase shift*  $t_i$  is given by the following formula (up to slight ambiguity to be resolved in a moment):

$$\operatorname{dn} t_i := \operatorname{dn} (t_i, k) = \begin{cases} \sqrt{f_i}, & \text{if } M < 1, \\ \frac{1}{\sqrt{f_i}}, & \text{if } M > 1. \end{cases}$$
 (11)

$$\begin{array}{c|ccc} & p_i q_i \in \mathbb{R}_{>0} & p_i q_i \in \mathbf{i} \mathbb{R}_{>0} & p_i q_i \in \mathbb{R}_{<0} \\ \hline \sigma_i < \pi & (0, \mathbf{i}K') & (K, K + \mathbf{i}K') & (2K, 2K + \mathbf{i}K') \\ \sigma_i > \pi & (2K, 2K + \mathbf{i}K') & (3K, 3K + \mathbf{i}K') & (0, \mathbf{i}K') \end{array}$$

Table 1: Phase shift intervals for different  $p_i q_i$  and  $\sigma_i$ .

Here, the value of the delta amplitude  $\operatorname{dn} t_i$  determines the value  $t_i$  up to the real half-period 2K. This ambiguity is resolved by Table 1, which shows intervals where  $t_i$  lies, depending on the values of  $p_i q_i$  and  $\sigma_i$ .

Note that there is a minor typographical error in the original definition of the equimodular elliptic type by Izmestiev [30, §3.3.1], specifically in the condition equating certain amplitudes; this was first noted by He [40]. Throughout this paper, we adopt the corrected conditions (6); the correction is purely notational and does not alter the classification framework.

We are ready to state the main theorem.

**Theorem 1.** Any elliptic QS-net has equimodular elliptic type and its flat angles satisfy

$$\delta_1 = \pi/2$$
 and  $\alpha_1, \beta_1, \gamma_1, \overline{\alpha}_1, \overline{\beta}_1, \overline{\gamma}_1, \overline{\delta}_1 \in (0, \pi).$  (12a)

Conversely, any  $\alpha_i$ ,  $\beta_i$ ,  $\gamma_i$ ,  $\delta_i$  satisfying (1), (2) and (12a) are flat angles of some flexible elliptic QS-net with a flexion given by

$$\cot \frac{\theta_1(t)}{2} = \frac{-t \sin \beta_1 \pm \sqrt{D(t)}}{\sin \bar{\delta}_1 \sin(\bar{\alpha}_1 - \beta_1) + t^2 \sin \bar{\alpha}_1 \sin(\bar{\delta}_1 - \beta_1)},$$

$$\cot \frac{\theta_2(t)}{2} = t,$$

$$\cot \frac{\theta_3(t)}{2} = \frac{t \sin \beta_1 \pm \sqrt{D(t)}}{\sin \bar{\delta}_1 \sin(\bar{\alpha}_1 - \beta_1) + t^2 \sin \bar{\alpha}_1 \sin(\bar{\delta}_1 - \beta_1)},$$

$$\cot \frac{\theta_4(t)}{2} = \pm \frac{\sqrt{D(t)}}{\sin \bar{\gamma}_1 \sin \bar{\delta}_1 + t^2 \sin(\bar{\gamma}_1 - \beta_1) \sin(\bar{\delta}_1 - \beta_1)},$$
(12b)

where t varies in some interval, the signs in  $\pm$  agree, and

$$D(t) := \left(\sin \sigma_1 \sin(\bar{\alpha}_1 - \beta_1) + t^2 \sin \bar{\alpha}_1 \sin \bar{\beta}_1\right) \times \left(t^2 \sin(\bar{\gamma}_1 - \beta_1) \sin(\bar{\delta}_1 - \beta_1) + \sin \bar{\gamma}_1 \sin \bar{\delta}_1\right).$$

We show that there exist two elliptic QS-nets with the same flat angles, one of which is flexible and the other one is not (see Proposition 3).

Furthermore, we establish an algebraic characterization of polyhedra of elliptic equimodular type with prescribed flat and dihedral angles of the central face. We aim at a system of algebraic equations, a minimal number of inequalities, and a few "discrete" conditions ensuring realizability in  $\mathbb{R}^3$ . The result is most concisely stated in terms of the parameters  $u, x_i, y_i, z_i$ leading to an efficient construction of polyhedra of elliptic equimodular type.

**Proposition 1.** Assume that  $\alpha_i$ ,  $\beta_i$ ,  $\gamma_i$ ,  $\delta_i$ ,  $\theta_i \in (0, \pi)$  satisfy condition (2) for each i = 1, ..., 4. Then a polyhedron with flat angles  $\alpha_i$ ,  $\beta_i$ ,  $\gamma_i$ ,  $\delta_i$  and dihedral angles  $\theta_i$  exists and has equimodular elliptic type, if and only if

$$\int \delta_1 + \delta_2 + \delta_3 + \delta_4 = 2\pi, \tag{13a}$$

$$u_1 = u_2 = u_3 = u_4 = u < 1, (13b)$$

$$x_1 = x_2, (13c)$$

$$x_3 = x_4, (13d)$$

$$y_1 = y_4, \tag{13e}$$

$$y_2 = y_3, (13f)$$

$$\cos \delta_i = \varepsilon_i \frac{1 - y_i z_i u - x_i z_i u + x_i y_i u}{2\sqrt{x_i y_i u(1 + z_i)(1 + u z_i)}},$$
(13g)

$$\begin{cases} \delta_{1} + \delta_{2} + \delta_{3} + \delta_{4} = 2\pi, & (13a) \\ u_{1} = u_{2} = u_{3} = u_{4} = u < 1, & (13b) \\ x_{1} = x_{2}, & (13c) \\ x_{3} = x_{4}, & (13d) \\ y_{1} = y_{4}, & (13e) \\ y_{2} = y_{3}, & (13f) \\ \cos \delta_{i} = \varepsilon_{i} \frac{1 - y_{i}z_{i}u - x_{i}z_{i}u + x_{i}y_{i}u}{2\sqrt{x_{i}y_{i}u(1 + z_{i})(1 + uz_{i})}}, & (13g) \\ \sin \theta_{i} \sin \theta_{i-1} = \varepsilon_{i} \frac{A_{i1} + A_{i2}y_{i}z_{i}u + A_{i3}x_{i}z_{i}u + A_{i4}x_{i}y_{i}u}{2\sqrt{x_{i}y_{i}u(1 + z_{i})(1 + uz_{i})}}, & (13h) \end{cases}$$

for each i = 1, ..., 4, and there exist  $e_1, e_2, e_3 \in \{+1, -1\}$  such that condition (7) holds, where  $\varepsilon_i$ ,  $x_i$ ,  $y_i$ ,  $z_i$ ,  $u_i$  are introduced in (3), (4), and

$$A_{ij} = 4\cos^2\left(\frac{\theta_i}{2} + \frac{\pi}{4}ij(j-1) + \frac{\pi j}{2}\right)\cos^2\left(\frac{\theta_{i-1}}{2} + \frac{\pi}{4}(i-1)j(j-1) + \frac{\pi j}{2}\right),\tag{13i}$$

for i, j = 1, ..., 4.

We see that this indeed is a system of algebraic equations in  $u, x_i, y_i$ , and  $z_i$ , and just one inequality u < 1, if  $\theta_i$  and  $\delta_i$  are prescribed.

All equations in the system have a simple geometric meaning. Equation (13a) is just the condition on the sum of angles of the planar quadrilateral  $A_1A_2A_3A_4$ . Equations (13b)–(13f) are just conditions (5) and (6). The set of four equations (13g) is a relation between the angles  $\delta_i$  and other parameters of the net introduced in (3) and (4). The set of four equations (13h) is the relation between the flat and dihedral angles, which is equivalent to Bricard's equations [30, Eq. (19)] for u < 1.

## 3. Proofs

We first prove Theorem 1 and then Proposition 1. The former requires three simple Lemmas 1-3, while the latter requires Lemmas 4-7. Henceforth, we use the notation provided in (3)-(11).

**Lemma 1.** If  $a_i, b_i, c_i, d_i$  are well-defined (that is,  $\sin \overline{\alpha}_i$ ,  $\sin \overline{\beta}_i$ ,  $\sin \overline{\gamma}_i$ ,  $\sin \overline{\delta}_i \neq 0$ ; see (4)) then

$$\begin{split} 1 - a_i b_i &= \frac{\sin \sigma_i \sin \left(\overline{\alpha}_i - \beta_i\right)}{\sin \overline{\alpha}_i \sin \overline{\beta}_i}, \qquad 1 - b_i c_i = \frac{\sin \sigma_i \sin \left(\overline{\gamma}_i - \beta_i\right)}{\sin \overline{\beta}_i \sin \overline{\gamma}_i}, \qquad 1 - b_i d_i = \frac{\sin \sigma_i \sin \left(\overline{\delta}_i - \beta_i\right)}{\sin \overline{\beta}_i \sin \overline{\delta}_i}, \\ c_i d_i - 1 &= \frac{\sin \sigma_i \sin \left(\overline{\alpha}_i - \beta_i\right)}{\sin \overline{\gamma}_i \sin \overline{\delta}_i}, \qquad a_i d_i - 1 = \frac{\sin \sigma_i \sin \left(\overline{\gamma}_i - \beta_i\right)}{\sin \overline{\alpha}_i \sin \overline{\delta}_i}, \qquad a_i c_i - 1 = \frac{\sin \sigma_i \sin \left(\overline{\delta}_i - \beta_i\right)}{\sin \overline{\alpha}_i \sin \overline{\gamma}_i}, \\ 1 - M_i &= \frac{\sin \sigma_i \sin \left(\overline{\alpha}_i - \beta_i\right) \sin \left(\overline{\gamma}_i - \beta_i\right) \sin \left(\overline{\delta}_i - \beta_i\right)}{\sin \overline{\alpha}_i \sin \overline{\beta}_i \sin \overline{\gamma}_i \sin \overline{\delta}_i}. \end{split}$$

*Proof.* The equalities are verified in Section 1 of the supplementary material (Criterion/helper.nb) [41].

**Lemma 2.** If  $\alpha_i$ ,  $\beta_i$ ,  $\gamma_i$ ,  $\delta_i \in (0, \pi)$  satisfy (2) then  $a_i$ ,  $b_i$ ,  $c_i$ ,  $d_i$  are well-defined and

$$a_i b_i, \ a_i c_i, \ a_i d_i, \ b_i c_i, \ b_i d_i, \ c_i d_i, \ M_i \neq 0, 1.$$

Proof. Condition (2) implies  $\sin \overline{\alpha}_i$ ,  $\sin \overline{\beta}_i$ ,  $\sin \overline{\gamma}_i$ ,  $\sin \overline{\delta}_i \neq 0$ . Thus  $a_i, b_i, c_i, d_i$  are well-defined. Then the right sides of equations in Lemma 1 do not vanish because  $\sigma_i$ ,  $\overline{\alpha}_i - \beta_i$ ,  $\overline{\gamma}_i - \beta_i$ ,  $\overline{\delta}_i - \beta_i \notin \pi \mathbb{Z}$  by (2). Since  $\alpha_i$ ,  $\beta_i$ ,  $\gamma_i$ ,  $\delta_i \in (0, \pi)$  it follows that  $a_ib_i$ ,  $a_ic_i$ ,  $a_id_i$ ,  $b_ic_i$ ,  $b_id_i$ ,  $c_id_i$ ,  $M_i \neq 0$ , see (4).

Remark 1. Conversely, one can show that condition (2) holds if and only if  $a_i, b_i, c_i, d_i$  are well-defined and  $M_i \neq 1$ .

**Lemma 3.** Replacement of numbers  $\alpha_i$ ,  $\beta_i$ ,  $\gamma_i$ ,  $\delta_i$  with their complements to  $\pi$  for all i = 1, ..., 4 preserves  $M_i$ ,  $r_i$ ,  $s_i$ ,  $f_i$  and conditions (2), (5)–(7).

*Proof.* First, for new angles  $\alpha_i^* := \pi - \alpha_i$ ,  $\beta_i^* := \pi - \beta_i$ ,  $\gamma_i^* := \pi - \gamma_i$ ,  $\delta_i^* := \pi - \delta_i$ , we have  $\alpha_i^* \pm \beta_i^* \pm \gamma_i^* \pm \delta_i^* = -\alpha_i \mp \beta_i \mp \gamma_i \mp \delta_i \pmod{2\pi}$ . Thus, condition (2) is preserved.

Second, since  $\sigma_i^{\star} = 2\pi - \sigma_i$ ,  $\overline{\alpha}_i^{\star} = \pi - \overline{\alpha}_i$ ,  $\overline{\beta}_i^{\star} = \pi - \overline{\beta}_i$ ,  $\overline{\gamma}_i^{\star} = \pi - \overline{\gamma}_i$ , and  $\overline{\delta}_i^{\star} = \pi - \overline{\delta}_i$ , by (4) it follows that new  $r_i^{\star} = \frac{\sin \alpha_i^{\star} \sin \delta_i^{\star}}{\sin \overline{\alpha}_i^{\star} \sin \overline{\delta}_i^{\star}} = \frac{\sin \alpha_i \sin \delta_i}{\sin \overline{\alpha}_i \sin \overline{\delta}_i} = r_i$ . Similarly,  $s_i^{\star} = s_i$ ,  $f_i^{\star} = f_i$ ,  $M_i^{\star} = M_i$  and hence (5) and (6) are preserved.

Third, since  $\sigma_i^* = 2\pi - \sigma_i$ ,  $r_i^* = r_i$ ,  $s_i^* = s_i$ ,  $f_i^* = f_i$ , and  $M_i^* = M_i$ , it follows that  $t_i^* - t_i = \pm 2K$  for all  $i = 1, \ldots, 4$  by (11), Table 1, and the 2K-periodicity of the delta amplitude dn(t). Since  $\pm 2K \pm 2K \pm 2K \pm 2K = 0 \pmod{4K}$  for any choice of signs in  $\pm$ , it follows that (7) is preserved.  $\square$ 

Remark 2. Lemma 3 remains true (with the same proof) if the replacement is performed for i = 2 and i = 4 only.

Proof of Theorem 1. First, any QS-net satisfies (12a). Indeed, by (1) we must have  $\delta_1 = \pi/2$  because  $\delta_2 + \delta_3 = \pi$ ,  $\delta_1 = \delta_4$ , and  $\delta_1 + \delta_2 + \delta_3 + \delta_4 = 2\pi$ . By Lemmas 2.1 and 4.1 from [30], we have  $\alpha_1, \beta_1, \gamma_1, \overline{\alpha}_1, \overline{\beta}_1, \overline{\gamma}_1, \overline{\delta}_1 \in (0, \pi)$ .

Let us prove that any elliptic QS-net has equimodular elliptic type. Since the net is elliptic, it follows that (2) is satisfied for all i = 1, ..., 4.

Directly from (4), we get  $M_1 = M_2 = M_3 = M_4 := M$ ,  $r_1 = r_2 = r_3 = r_4 := r$ ,  $s_1 = s_4$ , and  $s_2 = s_3$ . Thus, conditions (5) and (6) are satisfied.

Let us verify condition (7). Observe that  $\sigma_1 = \sigma_2 = \sigma_4$  and  $\sigma_3 = 2\pi - \sigma_1$ . Since  $\overline{\alpha}_1$ ,  $\overline{\beta}_1$ ,  $\overline{\gamma}_1$ ,  $\overline{\delta}_1 \in (0, \pi)$ , it follows that their permutations  $\overline{\alpha}_2$ ,  $\overline{\beta}_2$ ,  $\overline{\gamma}_2$ ,  $\overline{\delta}_2 \in (0, \pi)$  and  $\overline{\alpha}_4$ ,  $\overline{\beta}_4$ ,  $\overline{\gamma}_4$ ,  $\overline{\delta}_4 \in (0, \pi)$ . Since  $\alpha_3 = \pi - \delta_1$  and  $\sigma_3 = 2\pi - \sigma_1$ , it follows that  $\overline{\alpha}_3 = \pi - \overline{\delta}_1$  and hence  $\overline{\alpha}_3 \in (0, \pi)$ . Similarly,  $\overline{\beta}_3$ ,  $\overline{\gamma}_3$ ,  $\overline{\delta}_3 \in (0, \pi)$ .

Thus,  $r_i$ ,  $s_i$ ,  $f_i$ ,  $M_i \neq 1$  and are strictly positive for each i = 1, ..., 4 by Lemma 2 and (4). By Lemma 1 and (1), we have

$$(s_1-1)(s_2-1) = \frac{\sin\sigma_1\sin\left(\overline{\alpha}_1-\beta_1\right)}{\sin\overline{\gamma}_1\sin\overline{\delta}_1} \cdot \frac{\sin\sigma_2\sin\left(\overline{\alpha}_2-\beta_2\right)}{\sin\overline{\gamma}_2\sin\overline{\delta}_2} = -\frac{\sin^2\sigma_1\sin^2(\overline{\alpha}_1-\beta_1)}{\sin\overline{\alpha}_1\sin\overline{\beta}_1\sin\overline{\gamma}_1\sin\overline{\delta}_1} < 0.$$

Without loss of generality, we may assume that  $s_1 > 1 > s_2$  and  $\sigma_1 < \pi$ . Indeed, the case  $\sigma_1 > \pi$  is reduced to  $\sigma_1 < \pi$  using Lemma 3, and the case  $s_1 < 1 < s_2$  is reduced to  $s_1 > 1 > s_2$  using a cyclic permutation of indices and Remark 2.

Now, by (11), we have  $t_1 = t_4$  because  $f_1 = f_4 = \frac{\sin \alpha_1 \sin \gamma_1}{\sin \overline{\alpha}_1 \sin \overline{\gamma}_1} > 0$  and the delta amplitude dn(t) is injective on  $(mK, mK + \mathbf{i}K')$  for each  $m = 0, \dots, 3$ .

Since  $f_2 = \frac{\sin \beta_1}{\sin \overline{\beta_1} \sin \overline{\delta_1}}$  and  $M = f_1 f_2$ , it follows that

$$dn(t_2 - K) = \frac{k'}{dn t_2} = \begin{cases} \sqrt{M/f_2} = \sqrt{f_1} = dn t_1, & \text{for } M < 1, \\ \sqrt{f_2/M} = 1/\sqrt{f_1} = dn t_1, & \text{for } M > 1. \end{cases}$$

Thus  $\operatorname{dn}(t_2 - K) = \operatorname{dn} t_1$  and hence  $t_2 - K = t_1$  because, by Table 1, they both belong to either  $(0, \mathbf{i}K')$  (when r > 1) or  $(K, K + \mathbf{i}K')$  (when r < 1). Similarly,  $\operatorname{dn}(t_3 + K) = \operatorname{dn} t_1$ , hence  $t_3 - 3K = t_1$  (when  $t_3 + K = t_1$  (when  $t_3 - t_3 = t_$ 

Conversely, assume that  $\alpha_i$ ,  $\beta_i$ ,  $\gamma_i$ ,  $\delta_i$ , where i = 1, ..., 4, satisfy (12a), (2), and (1). Let us show that  $\alpha_i$ ,  $\beta_i$ ,  $\gamma_i$ ,  $\delta_i$  are flat angles of a flexible elliptic QS-net.

First, by (12a) and (1), we have  $\delta_1 + \delta_2 + \delta_3 + \delta_4 = 2\pi$  and  $M := M_1 > 0$ . By (2), the denominators in (12b) have finitely many roots.

Observe that there is always a non-empty interval for t such that D(t) > 0 in (12b). Indeed, since  $M = s_1 s_2$ , it follows by Lemma 1 that

$$D(t) = \sin \bar{\alpha}_1 \sin \bar{\beta}_1 \sin \bar{\gamma}_1 \sin \bar{\delta}_1 \left(1 - s_2 + t^2\right) \left(\frac{1 - M}{1 - s_2} t^2 + 1\right).$$

This expression is positive, for example, for  $t \in \mathbb{R}$  (when  $s_2 < 1$  and M < 1); for  $t \in \left(\sqrt{s_2 - 1}; \sqrt{\frac{s_2 - 1}{1 - M}}\right)$  (when  $s_2 > 1$  and M < 1); for  $t \in \left(\sqrt{s_2 - 1}, +\infty\right)$  (when  $s_2 > 1$  and M > 1); and for  $t \in \left(0, \sqrt{\frac{1 - s_2}{M - 1}}\right)$  (when  $s_2 < 1$  and M > 1).

For each t in those intervals, expressions (12b) satisfy Bricard's equations [30, Eq. (20)]; for an automated verification, see Section 0 of the supplimentary material (Criterion/helper.nb) [41]. Then there exists a polyhedron with the flat angles  $\alpha_i$ ,  $\beta_i$ ,  $\gamma_i$ ,  $\delta_i$  and cotangents of dihedral half-angles (12b) (the sufficiency of Bricard's equations and the condition  $\delta_1 + \delta_2 + \delta_3 + \delta_4 = 2\pi$  is well-known and reproved in Lemma 7 below in an equivalent form). In particular, any such polyhedron is flexible in  $\mathbb{R}^3$  and (12b) is a flexion. It is an elliptic QS-net by (2) and (1).

For the proof of Proposition 1, we need several inequalities on the parameters  $M_i$ ,  $r_i$ ,  $s_i$ ,  $f_i$ , also useful for the implementation of our algorithm.

**Lemma 4.** If  $\alpha_i$ ,  $\beta_i$ ,  $\gamma_i$ ,  $\delta_i \in (0, \pi)$  satisfy condition (2) and  $M_i > 0$ , then  $\overline{\alpha}_i$ ,  $\overline{\beta}_i$ ,  $\overline{\gamma}_i$ ,  $\overline{\delta}_i \in (0, \pi)$  and

$$r_i$$
,  $s_i$ ,  $f_i$ ,  $(r_i - 1)(r_i - M_i)$ ,  $(s_i - 1)(s_i - M_i)$ ,  $(f_i - 1)(f_i - M_i)$ ,  $(r_i - 1)(s_i - 1)(f_i - 1)(1 - M_i) > 0$ .

Proof. By Lemma 2, all the parameters in (4) are well-defined and we have  $r_i$ ,  $s_i$ ,  $f_i$ ,  $M_i \neq 0, 1$ . Using (4) and Lemma 1, we find the product  $(r_i - 1)(1 - M_i/r_i) = M_i \sin^2 \sigma_i \sin^2 (\overline{\gamma}_i - \beta_i)/(\sin \alpha_i \sin \beta_i \sin \gamma_i \sin \delta_i)$ . Hence, using (2) we get  $M_i r_i (r_i - 1)(r_i - M_i) > 0$ . Thus, since  $M_i > 0$ , we get  $r_i \in (0, \min\{1; M_i\}) \cup (\max\{1; M_i\}, +\infty)$ . Similarly,  $s_i$ ,  $f_i \in (0, \min\{1; M_i\}) \cup (\max\{1; M_i\}, +\infty)$ .

Since  $r_i$ ,  $s_i$ ,  $f_i$ ,  $M_i > 0$ , it follows that  $\operatorname{sgn} a_i = \operatorname{sgn} b_i = \operatorname{sgn} c_i = \operatorname{sgn} d_i$ . Then by (4), we have either  $\operatorname{sin} \overline{\alpha}_i$ ,  $\operatorname{sin} \overline{\beta}_i$ ,  $\operatorname{sin} \overline{\gamma}_i$ ,  $\operatorname{sin} \overline{\delta}_i > 0$  or  $\operatorname{sin} \overline{\alpha}_i$ ,  $\operatorname{sin} \overline{\beta}_i$ ,  $\operatorname{sin} \overline{\gamma}_i$ ,  $\operatorname{sin} \overline{\delta}_i < 0$ . Let us show that the latter is impossible. Indeed, otherwise  $\overline{\alpha}_i$ ,  $\overline{\beta}_i$ ,  $\overline{\gamma}_i$ ,  $\overline{\delta}_i \notin (0,\pi)$ . Since  $0 < \sigma_i < 2\pi$ , it follows that  $\overline{\alpha}_i$ ,  $\overline{\beta}_i$ ,  $\overline{\gamma}_i$ ,  $\overline{\delta}_i \in (-\pi,0) \cup (\pi,2\pi)$ . If a pair of angles, say,  $\overline{\alpha}_i$  and  $\overline{\beta}_i$ , belong to different intervals among  $(-\pi,0)$  and  $(\pi,2\pi)$  then  $|\overline{\alpha}_i-\overline{\beta}_i|=|\alpha_i-\beta_i|>\pi$ , contradicting  $\alpha_i$ ,  $\beta_i \in (0,\pi)$ . If all  $\overline{\alpha}_i$ ,  $\overline{\beta}_i$ ,  $\overline{\gamma}_i$ ,  $\overline{\delta}_i$  belong to the same interval, then  $-2\pi < \sigma_i < 0$  or  $2\pi < \sigma_i < 4\pi$  which contradicts  $0 < \sigma_i < 2\pi$ . Thus  $\operatorname{sin} \overline{\alpha}_i$ ,  $\operatorname{sin} \overline{\beta}_i$ ,  $\operatorname{sin} \overline{\gamma}_i$ ,  $\operatorname{sin} \overline{\delta}_i > 0$ , which implies  $\overline{\alpha}_i$ ,  $\overline{\beta}_i$ ,  $\overline{\gamma}_i$ ,  $\overline{\delta}_i \in (0,\pi)$ .

Finally, since  $\overline{\alpha}_i$ ,  $\overline{\beta}_i$ ,  $\overline{\gamma}_i$ ,  $\overline{\delta}_i \in (0, \pi)$ , it follows by Lemmas 1–2 that

$$(r_i - 1)(s_i - 1)(f_i - 1)(1 - M_i) = \frac{\sin^4 \sigma_i \sin^2(\overline{\alpha}_i - \beta_i) \sin^2(\overline{\gamma}_i - \beta_i) \sin^2(\overline{\delta}_i - \beta_i)}{\sin^3 \overline{\alpha}_i \sin \overline{\beta}_i \sin^3 \overline{\gamma}_i \sin^3 \overline{\delta}_i} > 0.$$

Remark 3. If (5) and (6) hold, then, multiplying the latter inequalities for all i = 1, ..., 4, we get  $(f_1 - 1)(f_2 - 1)(f_3 - 1)(f_4 - 1) > 0$ .

As a corollary, we deduce the existence of a polyhedron just from the inequalities  $M_i > 0$  and the condition  $\delta_1 + \delta_2 + \delta_3 + \delta_4 = 2\pi$ .

**Lemma 5.** Assume that  $\alpha_i$ ,  $\beta_i$ ,  $\gamma_i$ ,  $\delta_i \in (0, \pi)$  satisfy condition (2) for each  $i = 1, \ldots, 4$ . Then a polyhedron with flat angles  $\alpha_i$ ,  $\beta_i$ ,  $\gamma_i$ ,  $\delta_i$  exists if and only if  $\delta_1 + \delta_2 + \delta_3 + \delta_4 = 2\pi$  and  $M_i > 0$  for each  $i = 1, \ldots, 4$ .

*Proof.* ( $\Rightarrow$ ) If a polyhedron exists, then  $\delta_1 + \delta_2 + \delta_3 + \delta_4 = 2\pi$  and  $\overline{\alpha}_i$ ,  $\overline{\beta}_i$ ,  $\overline{\gamma}_i$ ,  $\overline{\delta}_i \in (0, \pi)$  by Lemmas 2.1 and 4.1 from [30]. Thus  $M_i > 0$  by (4).

( $\Leftarrow$ ) By Lemma 4 we have  $\overline{\alpha}_i$ ,  $\beta_i$ ,  $\overline{\gamma}_i$ ,  $\delta_i \in (0, \pi)$ . Since  $\alpha_i$ ,  $\beta_i$ ,  $\gamma_i$ ,  $\delta_i \in (0, \pi)$  as well and  $\delta_1 + \delta_2 + \delta_3 + \delta_4 = 2\pi$ , by Lemmas 2.1 and 4.1 from [30] there exists a polyhedron with flat angles  $\alpha_i$ ,  $\beta_i$ ,  $\gamma_i$ ,  $\delta_i$ , where  $i = 1, \ldots, 4$ .

The flat angles are expressed in terms of  $x_i, y_i, z_i, u$  as follows.

**Lemma 6.** Assume that  $\alpha_i$ ,  $\beta_i$ ,  $\gamma_i$ ,  $\delta_i \in (0,\pi)$  satisfy condition (2) and  $M_i > 0$  for each  $i = 1, \ldots, 4$ . Then

$$\cos \alpha_{i} = \varepsilon_{i} \frac{1 - y_{i}z_{i}u_{i} + x_{i}z_{i}u_{i} - x_{i}y_{i}u_{i}}{2\sqrt{x_{i}z_{i}u_{i}(1 + y_{i})(1 + u_{i}y_{i})}}, \qquad \cos \gamma_{i} = \varepsilon_{i} \frac{1 + y_{i}z_{i}u_{i} - x_{i}z_{i}u_{i} - x_{i}y_{i}u_{i}}{2\sqrt{y_{i}z_{i}u_{i}(1 + x_{i})(1 + u_{i}x_{i})}},$$

$$\cos \delta_{i} = \varepsilon_{i} \frac{1 - y_{i}z_{i}u_{i} - x_{i}z_{i}u_{i} + x_{i}y_{i}u_{i}}{2\sqrt{x_{i}y_{i}u_{i}(1 + z_{i})(1 + u_{i}z_{i})}}, \qquad \cos \sigma_{i} = \frac{1 - u_{i}(x_{i}y_{i} + x_{i}z_{i} + y_{i}z_{i} + 2x_{i}y_{i}z_{i})}{2\sqrt{x_{i}y_{i}z_{i}u_{i}^{2}(1 + x_{i})(1 + y_{i})(1 + z_{i})}},$$

$$\cos \beta_{i} = \varepsilon_{i} \frac{u_{i}(1 + x_{i})(1 + y_{i})(1 + z_{i}) + (1 + u_{i}x_{i})(1 + u_{i}y_{i})(1 + u_{i}z_{i}) - u_{i}x_{i}y_{i}z_{i}(u_{i} - 1)^{2}}{2\sqrt{u_{i}(1 + x_{i})(1 + y_{i})(1 + z_{i})(1 + u_{i}x_{i})(1 + u_{i}y_{i})(1 + u_{i}z_{i})}}.$$

Proof. Since  $a_i$ ,  $b_i$ ,  $c_i$ ,  $d_i$  and  $r_i$ ,  $s_i$ ,  $f_i$ ,  $M_i$ ,  $M_i/r_i$ ,  $M_i/s_i$ ,  $M_i/f_i \neq 0,1$  are well-defined (by Lemma 2) it follows that  $x_i$ ,  $y_i$ ,  $z_i \neq -1,0$  and  $u_i \neq 0,1$  are well-defined, and  $u_i x_i$ ,  $u_i y_i$ ,  $u_i z_i \neq -1$ . Next, since  $M_i > 0$  it follows by Lemma 4 that  $\overline{\alpha}_i$ ,  $\overline{\beta}_i$ ,  $\overline{\gamma}_i$ ,  $\overline{\delta}_i \in (0,\pi)$ . Finally, under the assumptions  $\alpha_i$ ,  $\beta_i$ ,  $\gamma_i$ ,  $\delta_i$ ,  $\overline{\alpha}_i$ ,  $\overline{\beta}_i$ ,  $\overline{\gamma}_i$ ,  $\overline{\delta}_i \in (0,\pi)$ , all the desired formulae are verified in Section 2 of the supplementary material (Criterion/helper.nb) [41].

Finally, we need the following characterization of possible flat and dihedral angles of an elliptic polyhedron (equivalent to Bricard's equations).

**Lemma 7.** Assume that  $\alpha_i$ ,  $\beta_i$ ,  $\gamma_i$ ,  $\delta_i$ ,  $\theta_i \in (0, \pi)$  satisfy condition (2) for each i = 1, ..., 4. Then a polyhedron with flat angles  $\alpha_i$ ,  $\beta_i$ ,  $\gamma_i$ ,  $\delta_i$  and dihedral angles  $\theta_i$  exists if and only if  $\delta_1 + \delta_2 + \delta_3 + \delta_4 = 2\pi$ ,  $M_i > 0$ , and equation (13h) holds for each i = 1, ..., 4.

*Proof.* We may restrict ourselves to the values  $\alpha_i$ ,  $\beta_i$ ,  $\gamma_i$ ,  $\delta_i$  satisfying  $\delta_1 + \delta_2 + \delta_3 + \delta_4 = 2\pi$  and  $M_i > 0$  because by Lemma 5, those conditions are necessary for the existence of a polyhedron.

Clearly, there exists a polyhedron with the given dihedral angles  $\theta_i$  and flat angles  $\alpha_i, \gamma_i, \delta_i$  (excluding  $\beta_i$ ) for i = 1, ..., 4. Denote by  $\widetilde{\beta}_i$ , where i = 1, ..., 4, the remaining flat angles of this polyhedron; see Figure 4. It suffices to prove that  $\widetilde{\beta}_i = \beta_i$  if and only if (13h) holds.

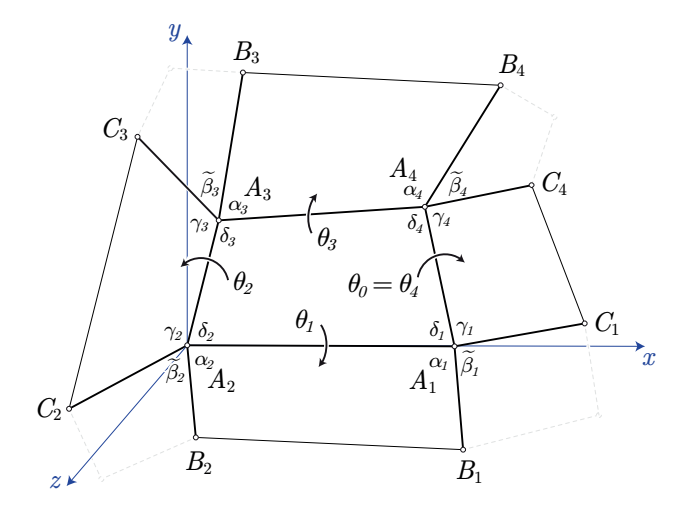


Figure 4: A polyhedron with some of the angles prescribed.

This follows from the following chain of equalities:

$$\frac{A_{i1} + A_{i2}y_i z_i u_i + A_{i3}x_i z_i u_i + A_{i4}x_i y_i u_i}{2\sqrt{x_i y_i u_i (1 + z_i)(1 + u_i z_i)}} = \\
= \varepsilon_i \left( \frac{\cos \beta_i - \cos \gamma_i (\cos \alpha_i \cos \delta_i + \cos \xi_i \sin \alpha_i \sin \delta_i)}{\sin \alpha_i \sin \gamma_i} - \frac{\cos \eta_i \sin \gamma_i (\cos \alpha_i \sin \delta_i - \cos \xi_i \sin \alpha_i \cos \delta_i)}{\sin \alpha_i \sin \gamma_i} \right) = \\
= \varepsilon_i \sin \theta_i \sin \theta_{i-1} + \varepsilon_i \frac{\cos \beta_i - \cos \widetilde{\beta}_i}{\sin \alpha_i \sin \gamma_i}.$$

Here  $A_{ij}$  are defined in (13i),  $\varepsilon_i = \operatorname{sgn}(\sin \sigma_i) \neq 0$ , and we denote  $\xi_i = \theta_i$ ,  $\eta_i = \theta_{i-1}$  for i = 1, 3 and  $\xi_i = \theta_{i-1}$ ,  $\eta_i = \theta_i$  for i = 2, 4. By the assumption  $M_i > 0$  and Lemma 4, we have  $\overline{\alpha}_i$ ,  $\overline{\beta}_i$ ,  $\overline{\gamma}_i$ ,  $\overline{\delta}_i \in (0, \pi)$ . Under the assumptions  $\alpha_i$ ,  $\beta_i$ ,  $\gamma_i$ ,  $\delta_i$ ,  $\overline{\alpha}_i$ ,  $\overline{\beta}_i$ ,  $\overline{\gamma}_i$ ,  $\overline{\delta}_i \in (0, \pi)$ , the first equality in the chain is checked in Section 3 of the supplementary material (Criterion/helper.nb) [41]. To prove the second equality, assume that i = 2 without loss of generality. Introduce the Cartesian coordinate system with the origin at  $A_2$  such that the face  $A_2A_3A_4A_1$  lies in the half-plane  $y \geq 0$  of the xy-plane and the ray  $A_2A_1$  is the x-axis as shown in Figure 4. The unit vectors  $\overrightarrow{e_1}$  and  $\overrightarrow{e_2}$  along

 $A_2B_2$  and  $A_2C_2$  equal

$$\vec{e_1} = \begin{pmatrix} \cos \alpha_2 \\ \sin \alpha_2 \cos \theta_1 \\ \sin \alpha_2 \sin \theta_1 \end{pmatrix} \quad \text{and} \quad \vec{e_2} = \begin{pmatrix} \cos \gamma_2 \cos \delta_2 + \sin \gamma_2 \cos \theta_2 \sin \delta_2 \\ \cos \gamma_2 \sin \delta_2 - \sin \gamma_2 \cos \theta_2 \cos \delta_2 \\ \sin \gamma_2 \sin \theta_2 \end{pmatrix}.$$

Since  $\overrightarrow{e_1} \cdot \overrightarrow{e_2} = \cos \widetilde{\beta}_2$ , the last equality in the chain follows.

Proof of Proposition 1. By Lemma 7, a polyhedron with flat angles  $\alpha_i$ ,  $\beta_i$ ,  $\gamma_i$ ,  $\delta_i$  and dihedral angles  $\theta_i$  exists if and only if conditions (13a), (13h), and  $u_i < 1$  hold for each i = 1, ..., 4. The polyhedron has elliptic equimodular type if and only if conditions (13b)–(13f) and (7) hold for some  $e_1, e_2, e_3 \in \{\pm 1\}$ , because (13b)–(13f) are equivalent to (5) and (6). For  $u_i < 1$ , equations (13g) are automatic by Lemma 6.

# 4. Algorithms and Examples

We now present several constructions of polyhedra of equimodular elliptic type, illustrated with examples. We start with closed-form examples, which are particular cases of Theorem 1, and establish their paradoxical properties. Then we construct an essentially different closed-form example by leveraging our findings, such as Proposition 1 and the lemmas in Section 3. This construction also demonstrates how the concept of quasi-symmetry was discovered. Next, we present a numerical search algorithm based on Proposition 1 and generate several numerical examples this way. Finally, we present a small-scale prototype.

## 4.1. Closed-form Examples

The most direct way to construct polyhedra of equimodular elliptic type is to apply Theorem 1. Let us discuss a specially chosen particular case.

**Example 4.1** (See Figure 5). Consider the polyhedron with flat angles

$$\alpha_1 = \alpha_4 = \delta_2 = 180^{\circ} - \delta_3 = 105^{\circ}, \quad \beta_1 = \beta_4 = \gamma_2 = 180^{\circ} - \gamma_3 = 15^{\circ},$$
  
 $\gamma_1 = \gamma_4 = \beta_2 = 180^{\circ} - \beta_3 = 120^{\circ}, \quad \delta_1 = \delta_4 = \alpha_2 = \alpha_3 = 90^{\circ},$ 

and the cotangents of dihedral half-angles

$$\cot \frac{\theta_1}{2} = \frac{(\sqrt{2} - \sqrt{6})t \pm \sqrt{2 + 6t^2 + 3t^4}}{1 + \sqrt{3} + 3t^2}, \quad \cot \frac{\theta_2}{2} = t,$$

$$\cot \frac{\theta_3}{2} = \frac{(\sqrt{6} - \sqrt{2})t \pm \sqrt{2 + 6t^2 + 3t^4}}{1 + \sqrt{3} + 3t^2}, \quad \cot \frac{\theta_4}{2} = \pm \frac{\sqrt{2 + 6t^2 + 3t^4}}{1 + \sqrt{3} + \sqrt{3}t^2},$$
(14)

where t is a parameter in the range  $(-\infty, +\infty)$  and the signs in  $\pm$  agree.

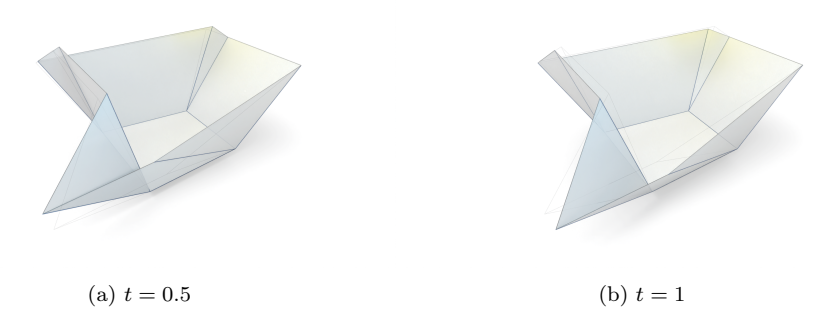


Figure 5: The QS-net in Example 4.1 at different values of parameter t. The sign "+" is chosen in each  $\pm$  in (14).

**Proposition 2.** The polyhedron in Example 4.1 belongs to equimodular elliptic type, does not belong to any other classes in Izmestiev's classification (even after switching the boundary strips), is flexible in  $\mathbb{R}^3$ , and a flexion is given by (14).

Hereafter, we refer to the classes introduced by Izmestiev [30, Section 3]. We do not recall their definition here, because most of them are excluded immediately. Switching the right boundary strip means replacement of  $\beta_1$ ,  $\beta_4$ ,  $\gamma_1$ ,  $\gamma_4$  with their complements to 180° and changing  $\theta_4$  to  $\theta_4 - 180$ °, leaving the other flat and dihedral angles unchanged [30, Section 2.5]. Switching the left, top, and bottom boundary strips is defined analogously.

Proof of Proposition 2. This proof is supplemented by a Mathematica notebook (Example1/helper1.nb) [41], which verifies every computation below.

First, we verify condition (2) by considering all possible choices of signs in  $\pm$ . Next, observe that  $\overline{\alpha}_1 = 60^\circ$ ,  $\overline{\beta}_1 = 150^\circ$ ,  $\overline{\gamma}_1 = 45^\circ$ ,  $\overline{\delta}_1 = 75^\circ \in (0, 180^\circ)$ . Thus by Theorem 1 our example is realizable and flexible in  $\mathbb{R}^3$ , with a flexion given by (14), and it has equimodular elliptic type.

Let us prove that this example belongs exclusively to this type and does not fall into any of the other classes introduced by Izmestiev, even after switching the boundary strips.

All the classes except for the orthodiagonal, conjugate-modular, linear compound, and trivial one are ruled out because they do not satisfy (2) for some i.

Since  $\cos \alpha_1 \cos \gamma_1 \neq 0 = \cos \beta_1 \cos \delta_1$ , it follows that the orthodiagonal class is ruled out. Switching the right boundary strip acts as replacement of  $\beta_1$ ,  $\beta_4$ ,  $\gamma_1$ ,  $\gamma_4$  with their complements to 180° and thus does not change this condition. Switching any number of the other boundary strips neither does.

Our example does *not* belong to the conjugate-modular class, because  $M_i = \sqrt{3} - 1 < 1$  for all i = 1, ..., 4 so that  $1/M_i + 1/M_{i+1} \neq 1$ . Switching the boundary strips does not transform our example to conjugate-modular class because it does not change  $M_i$ .

Our example does *not* belong to the trivial class, because none of the dihedral angles remains fixed during flexion by (14). Switching any number of the boundary strips does not transform our example to trivial class.

It remains to rule out the linear compound class. Recall that this class is defined by the condition that a component of the complexified configuration space of the polyhedron satisfies  $\cot \frac{\theta_1}{2}/\cot \frac{\theta_3}{2} = \mathrm{const}$  (or  $\cot \frac{\theta_1}{2}\cot \frac{\theta_3}{2} = \mathrm{const}$  after switching the boundary strips) [30, Section 3.5]. Here, the complexified configuration space is the set of complex solutions of the Bricard equations [30, Eq. (20)] in the variables  $w_1 := \cot \frac{\theta_1}{2}$ ,  $t := \cot \frac{\theta_2}{2}$ ,  $w_2 := \cot \frac{\theta_3}{2}$ ,  $t := \cot \frac{\theta_2}{2}$  (see Example1/helper1.nb in [41]):

$$\begin{cases} (1+\sqrt{3}+3t^2)w_1^2+2\sqrt{2}(\sqrt{3}-1)tw_1-t^2-\sqrt{3}+1=0,\\ (1+\sqrt{3}+3t^2)w_2^2-2\sqrt{2}(\sqrt{3}-1)tw_2-t^2-\sqrt{3}+1=0,\\ (2\sqrt{3}+(3+\sqrt{3})z^2)w_2^2-2(3+\sqrt{3})zw_2+2z^2+\sqrt{3}-1=0,\\ (2\sqrt{3}+(3+\sqrt{3})z^2)w_1^2-2(3+\sqrt{3})zw_1+2z^2+\sqrt{3}-1=0. \end{cases}$$

(Here, we have multiplied Bricard's equations by suitable constants. Also, more accurately, one should consider their bihomogenized versions, but this does not affect the following argument.)

Consider the first pair of equations. Solving them as quadratic equations in  $w_1$  and  $w_2$ , we parametrize the solutions by the first three expressions in (14) in a neighborhood of any point  $(w_1, t, w_2)$  such that  $2 + 6t^2 + 3t^4 \neq 0$  and  $1 + \sqrt{3} + 3t^2 \neq 0$ . Here, we choose any continuous branch of the square root in this neighborhood, and the signs in  $\pm$  need not agree. We conclude that one one-dimensional irreducible component of the solution set of the first pair of Bricard's equations satisfies  $w_1/w_2 = -1$ , and no other one-dimensional component satisfies  $w_1/w_2 =$ const nor  $w_1w_2 =$ const.

Analogously, one one-dimensional irreducible component of the solution set of the other pair of equations satisfies  $w_1/w_2 = +1$ , and no other one-dimensional irreducible component satisfies  $w_1/w_2 = \text{const}$  nor  $w_1w_2 = \text{const}$ 

const. As a result, no one-dimensional irreducible component of the solution set of all four equations satisfies  $w_1/w_2 = \text{const}$  nor  $w_1w_2 = \text{const}$ . So, our example does not belong to the linear compound class, even after switching the boundary strips.

Let us present another particular case of Theorem 1, which is paradoxical.

**Example 4.2** (See Figures 6–7). Let one polyhedron have flat angles

$$\alpha_1 = \alpha_4 = \delta_2 = 180^{\circ} - \delta_3 = 15^{\circ}, \qquad \beta_1 = \beta_4 = \gamma_2 = 180^{\circ} - \gamma_3 = 60^{\circ},$$
  
 $\gamma_1 = \gamma_4 = \beta_2 = 180^{\circ} - \beta_3 = 75^{\circ}, \qquad \delta_1 = \delta_4 = \alpha_2 = \alpha_3 = 90^{\circ},$ 

and the cotangents of dihedral half-angles

$$\cot \frac{\theta_1}{2} = \frac{\pm \sqrt{2}\sqrt{\sqrt{3}t^4 + 6t^2 + 2\sqrt{3}} - 2\sqrt{6}t}{2 - (\sqrt{3} + 1)t^2}, \quad \cot \frac{\theta_2}{2} = t,$$

$$\cot \frac{\theta_3}{2} = \frac{\pm \sqrt{2}\sqrt{\sqrt{3}t^4 + 6t^2 + 2\sqrt{3}} + 2\sqrt{6}t}{2 - (\sqrt{3} + 1)t^2}, \quad \cot \frac{\theta_4}{2} = \pm \frac{\sqrt{2}\sqrt{\sqrt{3}t^4 + 6t^2 + 2\sqrt{3}}}{(\sqrt{3} - 1)t^2 + 2},$$

$$(15a)$$

where  $t \neq -\sqrt{\sqrt{3}-1}$ ,  $\sqrt{\sqrt{3}-1}$  is a parameter and the signs in  $\pm$  agree.

Let the other polyhedron have the same flat angles and the cotangents of dihedral half-angles

$$\cot \frac{\theta_1}{2} = \cot \frac{\theta_3}{2} = 0, \quad \cot \frac{\theta_2}{2} = \sqrt{\frac{2}{3}} \cot \frac{\theta_4}{2} = \sqrt{1 + \sqrt{3}}.$$
 (15b)

**Proposition 3.** Two polyhedra in Example 4.2 have the same flat angles, but one of them is flexible (in  $\mathbb{R}^3$ ) and the other one is not (even in  $\mathbb{C}^3$ ).

The explanation for this apparent paradox is that the solution set of the system of Bricard's equations has components of different dimensions.

*Proof.* We use a supplementary material (Example2/helper2.nb) [41] for the proof, which verifies every computation below.

First, we verify condition (2) by considering all possible choices of signs in  $\pm$ . Next, we compute  $\overline{\alpha}_1 = 105^{\circ}$ ,  $\overline{\beta}_1 = 60^{\circ}$ ,  $\overline{\gamma}_1 = 45^{\circ}$ ,  $\overline{\delta}_1 = 30^{\circ} \in (0, 180^{\circ})$ . Thus, by Theorem 1, the first polyhedron is realizable and flexible in  $\mathbb{R}^3$ , with a flexion given by (15a).

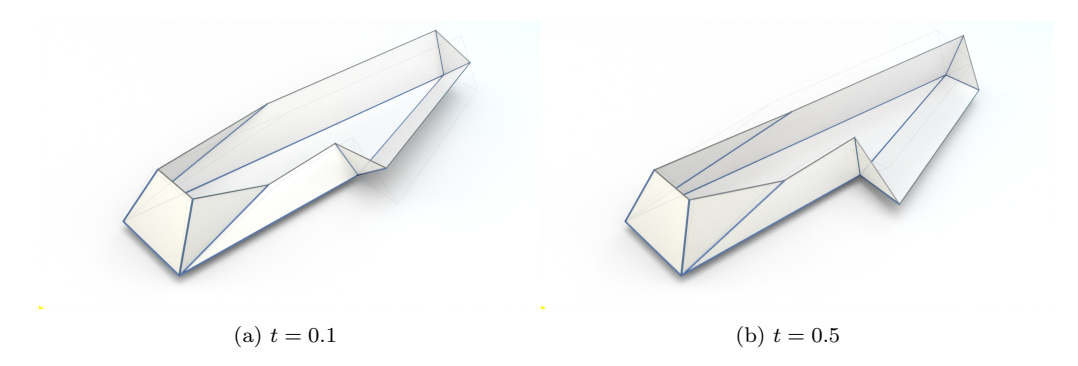


Figure 6: The first polyhedron in Example 4.2 at different values of parameter t. The sign "+" is chosen in each  $\pm$  in (15a).

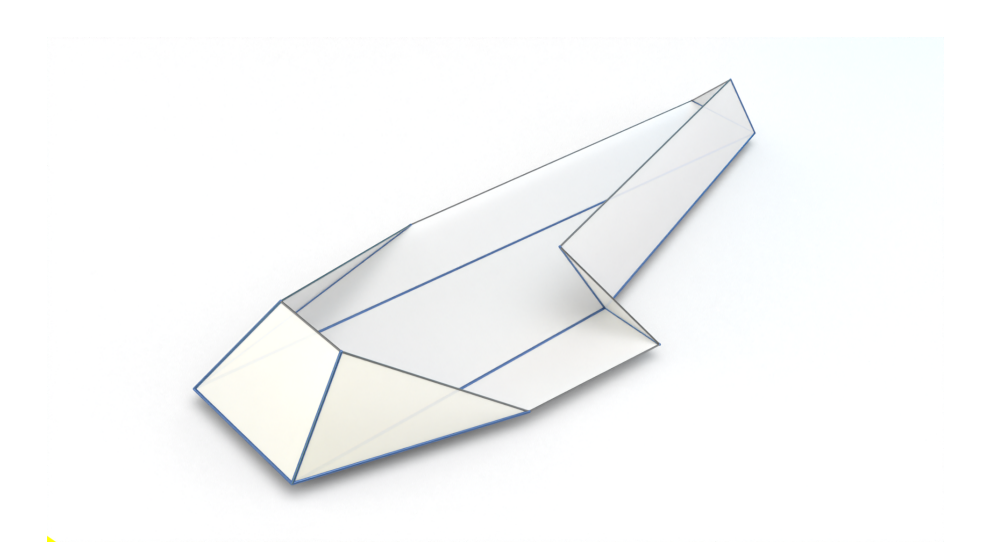


Figure 7: The second polyhedron in Example 4.2 for the fixed values of dihedral angles (15b). It has equimodular elliptic type but is not flexible.

To demonstrate the existence and non-flexibility of the second polyhedron, consider the system of Bricard's equations [30, Eq. (20)] in the variables  $w_1 := \cot \frac{\theta_1}{2}, t := \cot \frac{\theta_2}{2}, w_2 := \cot \frac{\theta_3}{2}, z := \cot \frac{\theta_4}{2}$  (see Example2/helper2.nb in [41]):

$$\frac{1}{\sqrt{3}} \left( \left( \sqrt{3} + 1 \right) t^2 - 2 \right) w_1^2 - 4\sqrt{2} t w_1 - \left( \sqrt{3} - 1 \right) t^2 + 2 = 0,$$

$$\frac{1}{\sqrt{3}} \left( \left( \sqrt{3} + 1 \right) t^2 - 2 \right) w_2^2 + 4\sqrt{2} t w_2 - \left( \sqrt{3} - 1 \right) t^2 + 2 = 0,$$

$$w_1^2 \left( z^2 - \sqrt{3} - 1 \right) + 2w_1 z + \left( \sqrt{3} - 1 \right) z^2 - 3 = 0,$$

$$w_2^2 \left( z^2 - \sqrt{3} - 1 \right) + 2w_2 z + \left( \sqrt{3} - 1 \right) z^2 - 3 = 0.$$

(We have multiplied Bricard's equations by suitable constants.) Since (15b) is a solution to the system, it follows that the second polyhedron exists.

Let us show that (15b) is an isolated solution to the system, so that the second polyhedron is not flexible (even in  $\mathbb{C}^3$ ). Consider the first pair of equations. Solving them as quadratic equations in  $w_1$  and  $w_2$ , we parametrize the complex solutions by the first three expressions in (15a) in a neighborhood of any point  $(w_1, t, w_2)$  such that  $t^4 + 2\sqrt{3}t^2 + 2 \neq 0$  and  $(\sqrt{3} + 1)t^2 - 2 \neq 0$ . Here, we choose any continuous branch of the square root in this neighborhood, and the signs in  $\pm$  need *not* agree.

The irreducible component of the solution set of the first pair of equations corresponding to the same choice of signs in  $\pm$  does not pass through the point  $(w_1, t, w_2) = (0, \sqrt{\sqrt{3} + 1}, 0)$  and can be ruled out.

Consider the other irreducible component, where the signs in  $\pm$  are opposite. On this component,  $w_1 = -w_2$ . Substituting this relation into the second pair of Bricard's equations, we conclude that  $w_1 = w_2 = 0$  or z = 0. In either case, we end up with a finite number of complex solutions to all four equations. Thus, solution (15b) is isolated.

Next, let us show how one can use the results from Sections 2–3 to construct different closed-form examples. For simplicity, we take  $\delta_i = \frac{\pi}{2}$  for each  $i = 1, \ldots, 4$ . We look over small values of u,  $z_i$  and try to express  $x_i$  and  $y_i$  using (13c)–(13g) (see Proposition 1) in order to satisfy conditions (5)–(7). Here, conditions (5) and (6) are easy to satisfy. However, satisfying condition (7) with explicit values of  $z_i$  is not so easy. For this reason, we introduce

an additional restriction on  $z_i$  and u, useful for Lemma 8 below. We use inequalities from Lemmas 4–5 to get more restrictions. Next, using Lemma 6, we calculate flat angles. Finally, we verify condition (2).

The simplest choice satisfying all those restrictions is  $u = \frac{1}{2}$ ,  $z_1 = 1$ ,  $z_2 = \frac{4}{3}$ ,  $z_3 = \frac{3}{2}$ ,  $z_4 = 2$ ,  $y_1 = \frac{1}{2}$ . It leads to the following example.

**Example 4.3** (See Figure 8). Consider the polyhedron with the cosines of flat angles

$$\cos \alpha_{1} = \frac{1}{\sqrt{5}}, \qquad \cos \beta_{1} = \frac{7}{5\sqrt{2}}, \qquad \cos \gamma_{1} = -\frac{1}{\sqrt{10}}, \qquad \cos \delta_{1} = 0,$$

$$\cos \alpha_{2} = \frac{1}{4\sqrt{11}}, \qquad \cos \beta_{2} = \frac{7\sqrt{7}}{4\sqrt{22}}, \qquad \cos \gamma_{2} = -\frac{1}{2\sqrt{2}}, \qquad \cos \delta_{2} = 0,$$

$$\cos \alpha_{3} = \frac{1}{4\sqrt{11}}, \qquad \cos \beta_{3} = \frac{7\sqrt{7}}{4\sqrt{22}}, \qquad \cos \gamma_{3} = \frac{1}{2\sqrt{2}}, \qquad \cos \delta_{3} = 0,$$

$$\cos \alpha_{4} = \frac{1}{\sqrt{5}}, \qquad \cos \beta_{4} = \frac{7}{5\sqrt{2}}, \qquad \cos \gamma_{4} = \frac{1}{\sqrt{10}}, \qquad \cos \delta_{4} = 0,$$

and the cotangents of dihedral half-angles

$$\cot \frac{\theta_1}{2} = t, \quad \cot \frac{\theta_2}{2} = \frac{5\sqrt{7}t \mp \sqrt{10(3t^2 - 1)(2 - 3t^2)}}{4 + 9t^2},$$

$$\cot \frac{\theta_3}{2} = \frac{1}{t}, \quad \cot \frac{\theta_4}{2} = \frac{6t \mp \sqrt{2(3t^2 - 1)(2 - 3t^2)}}{1 + 3t^2},$$
(16)

where t is a parameter in the range  $\left(\frac{1}{\sqrt{3}}, \frac{\sqrt{2}}{\sqrt{3}}\right)$  and the signs in  $\mp$  agree.

**Proposition 4.** The polyhedron from Example 4.3 belongs to equimodular elliptic type and linear compound type (after switching one of the boundary strips), does not belong to any other classes in Izmestiev's classification, is flexible in  $\mathbb{R}^3$ , and a flexion is given by (16).

We need a simple lemma.

**Lemma 8.** Let  $t_1$ ,  $t_2 \in (0, \mathbf{i}K')$  and  $k \in (0, 1)$ . Then  $t_1 + t_2 = \mathbf{i}K'$  if and only if  $k^2 \operatorname{sn}^2 t_1 \operatorname{sn}^2 t_2 = 1$ .

*Proof.* ( $\Rightarrow$ ) If  $t_1 + t_2 = \mathbf{i}K'$  then  $\operatorname{sn} t_2 = \operatorname{sn}(-t_1 + \mathbf{i}K') = -\frac{1}{k \operatorname{sn} t_1}$ , where  $\operatorname{sn} t_1 \neq 0$  as  $t_1 \in (0, \mathbf{i}K')$ . Thus  $k^2 \operatorname{sn}^2 t_1 \operatorname{sn}^2 t_2 = 1$ .

(⇐) Since  $\operatorname{sn} t_2$  is odd and injective on  $(-\mathbf{i}K', \mathbf{i}K')$ , it follows that the equation  $k^2 \operatorname{sn}^2 t_1 \operatorname{sn}^2 t_2 = 1$  implies  $t_2 = \mathbf{i}K' - t_1$ .

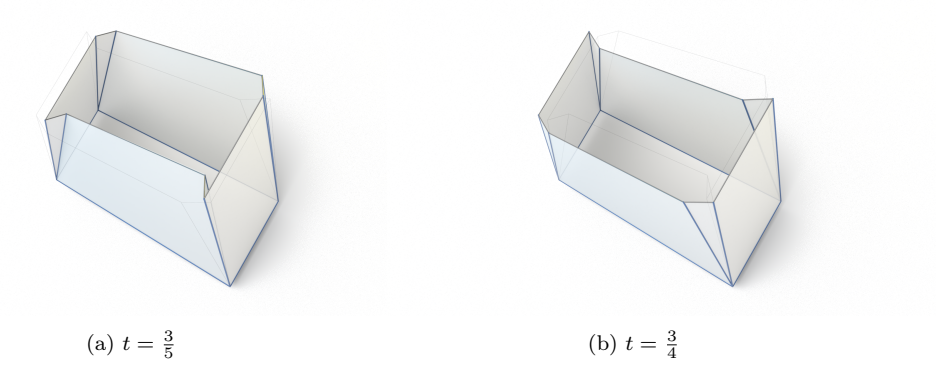


Figure 8: The polyhedron of equimodular elliptic type in Example 4.3 at different values of parameter t. The sign "-" is chosen in each  $\mp$  in (16).

Proof of Proposition 4. In this a computer-assistant proof, we use a supplementary material (Example3/helper3.nb) [41], which computes all the quantities  $r_i$ ,  $s_i$ ,  $f_i$ ,  $\sigma_i$ ,  $M_i$  and verifies every step below starting from expressing flat angles as inverse cosine function.

First, by Bricard's equations [30, Eq. (19)] our example is realizable and flexible in  $\mathbb{R}^3$  with the flexion given by (16), as verified in supplementary Mathematica notebook (Example3/helper3.nb) [41].

Second, we verify (2) by considering all possible choices of signs in  $\pm$ . Then using (4) we find  $r_1 = r_2 = \frac{4}{3}$ ,  $r_3 = r_4 = \frac{5}{2}$ ,  $s_1 = s_4 = 3$ ,  $s_2 = s_3 = \frac{11}{6}$ ,  $f_1 = 2$ ,  $f_2 = \frac{7}{4}$ ,  $f_3 = \frac{5}{3}$ ,  $f_4 = \frac{3}{2}$ ,  $M_1 = M_2 = M_3 = M_4 = M = \frac{1}{2}$ ,  $\sigma_1 = \arccos\left(-\frac{1}{\sqrt{2}}\right)$ ,  $\sigma_2 = \arccos\left(-\frac{3\sqrt{7}}{2\sqrt{22}}\right)$ ,  $\sigma_3 = \arccos\left(-\frac{2}{\sqrt{11}}\right)$ , and  $\sigma_4 = \arccos\left(-\frac{1}{\sqrt{5}}\right)$ . Thus (2), (5), and (6) hold.

Third, observe that  $\sigma_i < 180^{\circ}$  and  $p_i q_i \in \mathbb{R}_{>0}$ , see (10). Then by Table 1,  $t_i \in (0, \mathbf{i}K')$ , for each  $i = 1, \ldots, 4$ . Introduce  $t_5 := t_1$ . By (8) and (11), we get  $k^2 \operatorname{sn}^2 t_i \operatorname{sn}^2 t_{i+1} = \frac{(1-\operatorname{dn}^2 t_i)(1-\operatorname{dn}^2 t_{i+1})}{k^2} = \frac{(1-f_i)(1-f_{i+1})}{1-M} = 1$  for i = 2, 4. Then by Lemma 8, we have  $t_2 + t_3 = \mathbf{i}K'$  and  $t_1 + t_4 = \mathbf{i}K'$ . Hence  $t_1 - t_2 - t_3 + t_4 = 0$ , and (7) holds. Thus our example is of equimodular elliptic type.

Next, since  $\cot \frac{\theta_1}{2} \cot \frac{\theta_3}{2}$  is constant it follows that our example belongs to linear compound class after switching the upper boundary strip. Thus it is in the intersection of linear compound and equimodular elliptic classes.

Finally, analogously to the proof of Proposition 2, we check that this example does not fall into any of the other classes introduced by Izmestiev [30], even after switching the boundary strips.  $\Box$ 

## 4.2. Numerical Examples

To find concrete examples that satisfy the existence criterion in Proposition 1, we employ a two-phase numerical search-and-verification procedure. The input consists of dihedral angles  $\{\theta_i\}$  and flat angles  $\{\delta_i\}$  with all angles in  $(0,\pi)$  and  $\sum_{i=1}^4 \delta_i = 2\pi$  (Eq. (13a)), enforced by construction.

The unknowns are the parameters  $(u, x_1, x_3, y_1, y_2, z_1, z_2, z_3, z_4)$  We first incorporate symmetry relations (13b)–(13f) into (13g) and (13h). To remove sign ambiguities, we square (13g) and (13h). The resulting system has eight equations in the nine variables. We therefore augment it with a dummy equation 0 = 0 to obtain a square polynomial system.

To explore the (generally) non-convex solution set, we adopt a multi-start strategy, solving the system from many randomized initial guesses. These seeds are not chosen blindly: they are drawn from admissible domains implied by our theory, in particular Lemmas 2 and 4, as well as additional heuristic inequalities that bound the dihedral angles of realizable polyhedra. This significantly improves robustness and efficiency.

Each converged solution of the system is treated as a candidate and subjected to rigorous filtering. We discard non-physical  $(u \ge 1)$ , non-convergent, or duplicate solutions. Survivors are required to admit real-valued angles, i.e., the right sides of expressions in Lemma 6 must lie in [-1,1]. Finally, each candidate is validated against the original (unsquared) equations (13g) and (13h), as well as conditions (2) and (7) for some choice of  $\{e_j\}$ . At this step, it is convenient to treat  $\varepsilon_i$  and  $\sigma_i$  as additional variables and their definitions (4) as additional equations to be validated. The corresponding Python implementation is available in the supplementary material (Algorithm/numerical\_search.py) [41].

As for first example, we took as input

$$\delta_1 = 120^{\circ}, \qquad \delta_2 = 80^{\circ}, \qquad \delta_3 = 85^{\circ}, \qquad \delta_4 = 75^{\circ}, \\ \theta_1 = 130^{\circ}, \qquad \theta_2 = 140^{\circ}, \qquad \theta_3 = 125^{\circ}, \qquad \theta_4 = 135^{\circ}.$$

One admissible solution returned by our algorithm is presented in the following example; full-precision values (additional 12 decimal digits) are provided in the supplementary repository (Example4) [41].

**Example 4.4** (see Figure 9). Consider the polyhedron with flat angles

and the cotangents of dihedral half-angles

$$\cot \frac{\theta_{1}}{2} = t,$$

$$\cot \frac{\theta_{2}}{2} = \frac{0.99...t \mp 0.28...\sqrt{-4.34...t^{4} + 8.16...t^{2} - 1}}{t^{2} + 0.47...},$$

$$\cot \frac{\theta_{3}}{2} = \frac{-0.11...t \mp 0.98...\sqrt{-4.34...t^{4} + 8.16...t^{2} - 1}}{t^{2} - 1.74...},$$

$$\cot \frac{\theta_{4}}{2} = \frac{3.13...t \mp 0.75...\sqrt{-4.34...t^{4} + 8.16...t^{2} - 1}}{t^{2} + 1.93...},$$
(17)

where t is a parameter in the range (0.36..., 1.32...) and the signs in  $\mp$  agree.



Figure 9: Numerical example of a polyhedron of equimodular elliptic type at the state  $\theta_1 = 130^{\circ}$ ,  $\theta_2 = 140^{\circ}$ ,  $\theta_3 = 125^{\circ}$ ,  $\theta_4 = 135^{\circ}$ . See Example 4.4, where the minus sign is chosen in each  $\mp$ .

To verify that this example has the equimodular elliptic type (up to some tolerance), we processed it with the code in the supplementary material (Example4/helper4.nb) [41], following the same approach as in Examples 4.1–4.3. Condition (2) was verified by considering all possible choices of signs in  $\pm$ . We verified approximate equalities  $M_1 = M_2 = M_3 = M_4 = M = 0.92...$ ,  $r_1 = r_2 = 1.13...$ ,  $r_3 = r_4 = 0.68...$ ,  $s_1 = s_4 = 1.17...$ ,  $s_2 = s_3 = 1.09...$  with a further 10–14 digits available in the supplement. Period condition (7)

was validated numerically to a tolerance of  $10^{-15}$ . Bricard's equations [30, Eq. (19)] were satisfied for (17) to a tolerance of  $10^{-12}$ . In a sense, this means that the example is flexible in  $\mathbb{R}^3$  to tolerance  $10^{-12}$ .

Finally, we confirmed that the example belongs *exclusively* to the equimodular elliptic class (even after switching boundary strips), by the same approach used for Example 4.1; see (Example4/helper4.nb) [41].

In all preceding examples, we have M < 1. To complement these, we now consider a one with M > 1. While, for the same input data as in Example 4.4, our algorithm already returns several solutions with M > 1, we chose to test the effectiveness of the procedure on a different dataset. Specifically, we took as input

$$\delta_1 = 60^{\circ},$$
  $\delta_2 = 115^{\circ},$   $\delta_3 = 80^{\circ},$   $\delta_4 = 105^{\circ},$   $\theta_1 = 120^{\circ},$   $\theta_2 = 140^{\circ},$   $\theta_3 = 110^{\circ},$   $\theta_4 = 130^{\circ}$ 

and obtained an admissible solution reported in Example 4.5. Full-precision values (additional 12 decimal digits) are provided in the supplementary repository (Example5) [41].

**Example 4.5** (See Figure 10). Consider the polyhedron with flat angles

and the cotangents of dihedral half-angles

$$\cot \frac{\theta_{1}}{2} = t,$$

$$\cot \frac{\theta_{2}}{2} = \frac{-0.21... t \pm 0.29... \sqrt{-2.70... t^{4} + 2.67... t^{2} + 1}}{t^{2} + 0.33...},$$

$$\cot \frac{\theta_{3}}{2} = \frac{0.54... t \pm 0.31... \sqrt{-2.70... t^{4} + 2.67... t^{2} + 1}}{t^{2} + 0.67...},$$

$$\cot \frac{\theta_{4}}{2} = \frac{-0.39... t \pm 0.43... \sqrt{-2.70... t^{4} + 2.67... t^{2} + 1}}{t^{2} + 0.35...},$$
(18)

where t is a parameter in the range (0, 1.13...) and the signs in  $\pm$  agree.

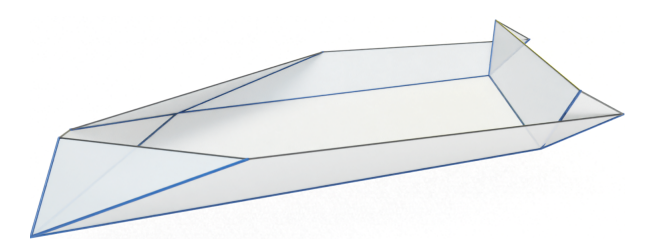


Figure 10: The numerical example of a polyhedron of equimodular elliptic type in Example 4.5 at the state  $\theta_1 = 120^{\circ}$ ,  $\theta_2 = 140^{\circ}$ ,  $\theta_3 = 110^{\circ}$ ,  $\theta_4 = 130^{\circ}$ . The sign "+" is chosen in each  $\pm$  in (18).

To verify that this example has equimodular elliptic type (to numerical tolerance), we processed it with the supplementary Mathematica notebook (Example5/helper5.nb) [41], following the same approach as in previous examples. Condition (2) was verified by considering all possible choices. We verified the approximate equalities  $M_1 = M_2 = M_3 = M_4 = M = 1.22...$ ,  $r_1 = r_2 = 0.71...$ ,  $r_3 = r_4 = 0.88...$ ,  $s_1 = s_4 = 0.58...$ ,  $s_2 = s_3 = 0.80...$  with a further 11–13 digits available in the supplement. Period condition (7) was validated numerically to a tolerance of  $10^{-15}$ . In addition, Bricard's equations were satisfied for (18) to a tolerance of  $10^{-12}$ .

Furthermore, this example does *not* belong to the conjugate-modular class because  $M_1 = M_2 = M_3 = M_4 = M$  and  $M \neq 2$ ; switching boundary strips does not affect  $M_i$  and thus does not change this conclusion. As in Example 4.1, we verified that the example does *not* belong to any other classes (even after switching boundary strips); see (Example5/helper5.nb) [41].

Remark 4. In our simulations, Examples 4.3–4.5 are non-self-intersecting, if we choose the upper sign in each  $\mp$  and  $\pm$ , and become self-intersecting, otherwise. Reproducible Python scripts are provided in the example folders of the supplementary repository [41].

### 4.3. Small-scale Prototype

We show that the proposed mechanisms can be successfully realized in practice by building the small-scale (about  $150 \times 150 \times 100 \text{ mm}^3$ ) shown in Figure 11 of our QS-net, which has been previously presented in Figure 5. Unlike Maleczek et al. [42] and others, we opted against rapid prototyping and the use of plastics, as these materials can introduce significant tolerances and undesired flexibility. Instead, we selected stainless steel for the fabrication of our model. Its motion is purely a consequence of its geometry,

with no flexibility, deformation, or loose fitting of the material contributing to movement.

The mechanism is constructed from a 0.5 mm thick laser-cut hard-rolled stainless steel sheet (1.4404), CNC-cut cold-drawn stainless steel seamless capillary pipe (1.4301) with an outer diameter of 2.5 mm and a wall thickness of 0.5 mm, and straightened carbon spring steel wire (1.1200) with a diameter of 1.5 mm. The joint knuckles were fusion pulse TIG-welded to the edges of the laser-cut quadrilaterals. The fit between the knuckle and the pin at the joints is H10/h8 (knuckle inner diameter 1.5 mm -0/+50 µm, pin diameter 1.5 mm +0/-14 µm). The resulting mechanism is both stiff and smooth, with only a single degree of motion and no backlash or wiggle.



Figure 11: Illustration of several configurations of our fabricated flexible QNS. Photos (top) and corresponding renderings (bottom) are shown.

#### 5. Discussion

In this work, we fill a notable gap in the classification of flexible Kokotsakis polyhedra with quadrangular base by providing the first explicit constructions of the equimodular elliptic type – most directly via Theorem 1 (the QS-net) – and by deriving an explicit algebraic characterization (Proposition 1) that links flat and dihedral angles through the variables  $(u, x_i, y_i, z_i)$  and the relations (13b)–(13h). Although the definition of quasi-symmetric nets is elementary and direct, the path to this definition was via the implementation and analysis of the more complicated algebraic characterization.

Our results complement Izmestiev's algebraic classification [30], which identified this type but did not provide concrete realizations. Beyond existence, we establish flexibility in  $\mathbb{R}^3$  by providing closed-form flexions for

analytic examples (Examples 4.1–4.3), presenting numerical instances validated to tight tolerances (Examples 4.4–4.5), and giving systematic evidence that these instances lie *exclusively* within the equimodular elliptic class even after switching the boundary strips (Examples 4.1, 4.4–4.5). Importantly, our examples cover both cases M < 1 and M > 1, indicating the breadth of realizable behavior within this class. Across our examples we observed both non-self-intersecting motion and self-intersection (see Remark 4).

For the numerical results, Bricard's equations [30, Eq. (19)] are satisfied to  $10^{-12}$ , period condition (7) to  $10^{-15}$ , moduli condition (5) to  $10^{-14}$  or better, amplitudes condition (6) to  $10^{-12}$  or better, and condition (2) is satisfied with even better precision. These tolerances are more than sufficient for constructing physical prototypes. All scripts and notebooks are released to support full reproducibility [41].

From a CAD perspective, Theorem 1 offers an immediate source of simple, closed-form designs (QS-nets) with prescribed flat-angle relations. More generally, Proposition 1 is directly actionable: it reduces the synthesis of mechanisms of equimodular elliptic type to solving a structured algebraic system with simple symmetry constraints (13b)–(13f) and two core relations - a face-compatibility equation for  $\delta_i$  (13g) and a kinematic equation for the dihedral angles (13h). This enables (i) fast feasibility checks during interactive modeling, (ii) inverse design by prescribing partial angle data and solving for remaining parameters, and (iii) automatic rejection of designs drifting into non-elliptic regimes (violations of (2)) or non-physical solutions. The numerical pipeline (Section 4.2) is tailored for this workflow: it uses theory-informed sampling (Lemmas 2 and 4) to initialize solvers; candidates are verified against the unsquared equations and consistent sign patterns  $\{\varepsilon_i\}, \{e_j\}$ ; and the period condition (7) is certified at prescribed tolerances. Together with our constructive routines for coordinate formulae, edge and angle generation, and construction and interactive flexion (see Appendix/appendix.pdf [41]), this yields a robust pipeline from CAD to physical prototype.

Future work will address the open problems above, including the following directions: to extend the theory and algorithms from  $3 \times 3$  nets to general  $m \times n$  nets; to investigate whether all polyhedra of equimodular elliptic type are flexible in  $\mathbb{R}^3$  for some range of their dihedral angles and, if so, to derive explicit flexion formulae; to seek simpler reformulations of period condition (7) in terms of elementary functions for faster verification; and to explore potential hidden symmetries within the equimodular elliptic type.

#### 6. Conclusion

To summarize, we addressed a long–standing gap in the theory of flexible mechanisms by providing the first explicit constructions and an algebraic characterization of quadrangular Kokotsakis polyhedra of the equimodular elliptic type. Building on Izmestiev's abstract framework, we translated the classification into a polynomial system that directly links flat and dihedral angles. This system – formulated in Proposition 1 and complemented by the constructive Theorem 1 – serves as the central theoretical contribution and enables a rigorous, constructive pathway to identify members of this class.

On this foundation, we showed conclusively that the equimodular elliptic class is physically realizable. We presented the first closed-form examples together with numerical instances discovered via a robust search-and-verify pipeline. For all of these, we established flexibility in  $\mathbb{R}^3$ , provided motion parameterizations, and verified that most of them belong exclusively to the equimodular elliptic class, even after switching the boundary strips. The examples include non-self-intersecting realizations and span both regimes M < 1 and M > 1, underscoring the breadth of attainable behavior.

Beyond these foundational contributions, we have developed and validated a complete computational pipeline that bridges the gap between theory and practice. The numerical search-and-verification algorithm, informed by our analytical results, provides an effective tool for discovering new mechanisms and can be integrated directly into CAD workflows for the inverse design and simulation of flexible structures.

The presented results resolve several open questions and simultaneously lay the groundwork for new avenues of inquiry, such as extending the framework to larger nets. In providing the first tangible examples and a clear pathway for their design and construction, this research enriches the classification of flexible polyhedra and offers a new family of mechanisms for applications in architectural geometry, robotics, and deployable systems. In future work along different trajectories, we could investigate the dynamic behavior and stability of these flexible mechanisms under external loads, drawing on techniques such as exponential integration [43, 44] for stiff problems [45, 46]. There is also potential to explore the application of graph learning [47]. Also, the exploration of flexible molds based on such mechanisms [48] could lead to novel fabrication techniques.

#### References

- [1] F. Escrig, J. P. Valcarcel, Geometry of expandable space structures, International Journal of Space Structures 8 (1-2) (1993) 71–84.
- [2] S. Calatrava, Zur faltbarkeit von fachwerken, Ph.D. thesis, ETH Zurich (1981).
- [3] Z. Li, G. Nawratil, F. Rist, M. Hensel, Invertible paradoxic loop structures for transformable design, in: Computer Graphics Forum, Vol. 39, Wiley Online Library, 2020, pp. 261–275.
- [4] E. Demaine, J. O'Rourke, Geometric Folding Algorithms, Cambridge Univ. Press, 2007.
- [5] T. A. Evans, R. J. Lang, S. P. Magleby, L. L. Howell, Rigidly foldable origami gadgets and tessellations, Royal Society Open Science 2 (2015) #150067, 2–18.
- [6] T. A. Evans, R. J. Lang, S. P. Magleby, L. L. Howell, Ridigly foldable origami twists, in: Origami <sup>6</sup>, Vol. 1, American Math. Soc, 2015, pp. 119–130.
- [7] C. Jiang, K. Mundilova, F. Rist, J. Wallner, H. Pottmann, Curve-pleated structures, ACM Trans. Graph. 38 (6) (2019) 169:1–13.
- [8] K. Song, X. Zhou, S. Zang, H. Wang, Z. You, Design of rigid-foldable doubly curved origami tessellations based on trapezoidal crease patterns, Proc. R. Soc. A 473 (2017) #20170016, 1–18.
- [9] T. Tachi, Generalization of rigid foldable quadrilateral mesh origami, J. Int. Ass. Shell & Spatial Structures 50 (2009) 173–179.
- [10] T. Tachi, Geometric considerations for the design of rigid origami structures, in: Q. Zhang, L. Yang, Y. Hu (Eds.), Proceedings of the International Association for Shell and Spatial Structures (IASS) Symposium 2010: Spatial Structures—Temporary and Permanent, China Architecture & Building Press, Shanghai, 2010, pp. 771–782.
- [11] T. Tachi, Freeform rigid-foldable structure using bidirectionally flat-foldable planar quadrilateral mesh, in: C. Ceccato, et al. (Eds.), Advances in Architectural Geometry 2010, Springer, 2010, pp. 87–102.

- [12] T. Tachi, G. Epps, Designing one-DOF mechanisms for architecture by rationalizing curved folding, in: Y. Ikeda (Ed.), Proc. ALGODE Symposium, Arch. Institute Japan, Tokyo, 2011, p. 14 pp.
- [13] T. Tachi, Composite rigid-foldable curved origami structure, in: F. Escrig, J. Sanchez (Eds.), Proc. 1st Transformables Conf., Starbooks, Sevilla, 2013, p. 6 pp.
- [14] S. Callens, A. Zadpoor, From flat sheets to curved geometries: Origami and kirigami approaches, Materials Today 21 (3) (2018) 241–264.
- [15] P. Dieleman, N. Vasmel, S. Waitukaitis, M. van Hecke, Jigsaw puzzle design of pluripotent origami, Nature Physics 16 (1) (2020) 63–68.
- [16] L. H. Dudte, E. Vouga, T. Tachi, L. Mahadevan, Programming curvature using origami tessellations, Nature materials 15 (5) (2016) 583.
- [17] C. Jiang, F. Rist, H. Wang, J. Wallner, H. Pottmann, Shape-morphing mechanical metamaterials, Computer Aided Design 143 (2022).
- [18] M. Konaković, K. Crane, B. Deng, S. Bouaziz, D. Piker, M. Pauly, Beyond developable: Computational design and fabrication with auxetic materials, ACM Trans. Graph. 35 (4) (2016) 89:1–11.
- [19] M. Konaković-Luković, J. Panetta, K. Crane, M. Pauly, Rapid deployment of curved surfaces via programmable auxetics, ACM Trans. Graph. 37 (4) (2018) 106:1–13.
- [20] J. L. Silverberg, A. A. Evans, L. McLeod, R. C. Hayward, T. Hull, C. D. Santangelo, I. Cohen, Using origami design principles to fold reprogrammable mechanical metamaterials, science 345 (6197) (2014) 647–650.
- [21] A.-L. Cauchy, Recherche sur les polyédres premier mémoire, Journal de l'École Polytechnique 9 (1813) 7–25, in French.
- [22] R. Bricard, Mémoire sur la théorie de l'octaèdre articulé, Journal de Mathématiques pures et appliquées 3 (1897) 113–148.
- [23] A. Kokotsakis, Über bewegliche Polyeder, Math. Ann. 107 (1933) 627–647.

- [24] R. Sauer, H. Graf, Über Flächenverbiegung in Analogie zur Verknickung offener Facettenflache, Math. Ann. 105 (1931) 499–535.
- [25] H. Stachel, A kinematic approach to Kokotsakis meshes, Comp. Aided Geom. Design 27 (2010) 428–437.
- [26] G. Nawratil, Reducible compositions of spherical four-bar linkages with a spherical coupler component, Mechanism and Machine Theory 46 (5) (2011) 725–742.
- [27] G. Nawratil, Reducible compositions of spherical four-bar linkages without a spherical coupler component, Mechanism and machine theory 49 (2012) 87–103.
- [28] W. Schief, A. Bobenko, T. Hoffmann, On the integrability of infinitesimal and finite deformations of polyhedral surfaces, in: A. Bobenko, et al. (Eds.), Discrete differential geometry, Vol. 38 of Oberwolfach Seminars, Springer, 2008, pp. 67–93.
- [29] O. N. Karpenkov, On the flexibility of Kokotsakis meshes, Geometriae Dedicata 147 (1) (2010) 15–28.
- [30] I. Izmestiev, Classification of flexible Kokotsakis polyhedra with quadrangular base, Int. Math. Res. Not. 2017 (3) (2017) 715–808.
- [31] Y. Liu, Y. Ouyang, D. L. Michels, On the algebraic classification of non-singular flexible Kokotsakis polyhedra, arXiv (2401.14291) (2024).
- [32] V. A. Gor'kavyi, A. D. Milka, Birosettes are model flexors, Ukr. Math. J. 70 (7) (2018) 885–904.
- [33] C. Jiang, D. Lyakhov, F. Rist, H. Pottmann, J. Wallner, Quad mesh mechanisms, ACM Trans. Graph. 43 (6) (2024) 243:1–243:17, proc. SIG-GRAPH Asia.
- [34] O. Pirahmad, H. Pottmann, M. Skopenkov, Area preserving Combescure transformations, Results Math 80 (27) (2025).
- [35] O. Pirahmad, H. Pottmann, M. Skopenkov, Flexible polyhedral nets in isotropic geometry, arXiv preprint arXiv:2504.15060 (2025).

- [36] K. Yorov, B. Wang, M. Skopenkov, H. Pottmann, C. Jiang, Solving Euclidean problems by isotropic initialization, arXiv (2506.01726) (2025).
- [37] I. Erofeev, G. Ivanov, Orthodiagonal anti-involutive Kokotsakis polyhedra, Mechanism and Machine Theory 146 (2020) 103713.
- [38] A. Aikyn, Y. Liu, D. A. Lyakhov, F. Rist, H. Pottmann, D. L. Michels, Flexible Kokotsakis meshes with skew faces: Generalization of the orthodiagonal involutive type, Computer-Aided Design 168 (2024) 103669.
- [39] E. A. Morozov, Symmetries of 3-polytopes with fixed edge lengths, Sib. Electron. Math. Rep. 17 (2020) 1580–1587.
- [40] Z. He, On the foldability of rigid origami, Ph.D. thesis, University of Cambridge, Cambridge, UK, supervisor: Simon D. Guest; Advisor: Allan McRobie; Department of Engineering (Aug. 2021).
- [41] A. Nurmatov, M. Skopenkov, F. Rist, J. Klein, D. L. Michels, Quasi-symmetric nets: A constructive approach to the equimodular elliptic type of Kokotsakis polyhedra: Code and notebooks, https://github.com/nurmaton/qs-nets (2025).
- [42] R. Maleczek, K. Sharifmoghaddam, G. Nawratil, Rapid prototyping for non-developable discrete and semi-discrete surfaces with an overconstrained mobility, in: Proceedings of IASS Annual Symposia, Vol. 2022, International Association for Shell and Spatial Structures (IASS), 2022, pp. 1–12.
- [43] D. L. Michels, G. A. Sobottka, A. G. Weber, Exponential integrators for stiff elastodynamic problems, ACM Trans. Graph. 33 (1) (Feb. 2014).
- [44] D. L. Michels, J. P. T. Mueller, Discrete computational mechanics for stiff phenomena, in: SIGGRAPH ASIA 2016 Courses, SA '16, Association for Computing Machinery, New York, NY, USA, 2016.
- [45] D. L. Michels, J. P. T. Mueller, G. A. Sobottka, A physically based approach to the accurate simulation of stiff fibers and stiff fiber meshes, Computers & Graphics 53 (2015) 136–146.
- [46] D. L. Michels, V. T. Luan, M. Tokman, A stiffly accurate integrator for elastodynamic problems, ACM Trans. Graph. 36 (4) (Jul. 2017).

- [47] H. Shao, T. Kugelstadt, T. Hädrich, W. Palubicki, J. Bender, S. Pirk, D. L. Michels, Accurately solving rod dynamics with graph learning, in: M. Ranzato, A. Beygelzimer, Y. Dauphin, P. Liang, J. W. Vaughan (Eds.), Advances in Neural Information Processing Systems, Vol. 34, Curran Associates, Inc., 2021, pp. 4829–4842.
- [48] F. Rist, Z. Wang, D. Pellis, M. Palma, D. Liu, E. Grinspun, D. L. Michels, A flexible mold for facade panel fabrication, ACM Trans. Graph. 43 (6) (Nov. 2024).

# Acknowledgements

This research has been supported by the baseline funding of the KAUST Computational Sciences Group.